

1 Spatial and temporal dynamics of suspended sediment concentrations in coastal waters of South  
2 China Sea, off Sarawak, Borneo: Ocean colour remote sensing observations and analysis

3 **Jenny Choo<sup>1</sup>, Nagur Cherukuru<sup>2</sup>, Eric Lehmann<sup>2</sup>, Matt Paget<sup>2</sup>, Aazani Mujahid<sup>3</sup>, Patrick Martin<sup>4</sup>, Moritz Müller<sup>1</sup>**

4 <sup>1</sup>Swinburne University of Technology, Faculty of Engineering, Computing and Science, Jalan Simpang Tiga, 93350 Kuching,  
5 Sarawak, Malaysia.

6 <sup>2</sup>Commonwealth Scientific and Industrial Research Organization (CSIRO), Canberra ACT 2601, Australia.

7 <sup>3</sup>Faculty of Resource Science & Technology, University Malaysia Sarawak, Kota Samarahan 94300, Sarawak, Malaysia.

8 <sup>4</sup>Asian School of the Environment, Nanyang Technological University, 639798, Singapore.

9

10 *Correspondence to:* Jenny Choo (JChoo@swinburne.edu.my/jccy89@gmail.com)

11

12 **Abstract**

13 High-quality ocean colour observations are increasingly accessible to support various monitoring and  
14 research activities for water quality measurements. In this paper, we present a newly developed  
15 regional total suspended solids (TSS) empirical model using MODIS-Aqua's Rrs(530) and Rrs(666)  
16 reflectance bands to investigate the spatial and temporal variation of TSS dynamics along the  
17 southwest coast of Sarawak, Borneo, with the application of the Open Data Cube (ODC) platform. The  
18 performance of this TSS retrieval model was evaluated using error metrics (bias = 1.0, MAE = 1.47, and  
19 RMSE = 0.22 in mg/L) with a log<sub>10</sub> transformation prior to calculation, as well as a k-fold cross  
20 validation technique. The temporally averaged map of TSS distribution, using daily MODIS-Aqua  
21 satellite datasets from 2003 until 2019, revealed large TSS plumes detected particularly in the Lupar  
22 and Rajang coastal areas on a yearly basis. The average TSS concentration in these coastal waters was  
23 in the range of 15 – 20 mg/L. Moreover, the spatial map of TSS coefficient of variation (CV) indicated  
24 strong TSS variability (approximately 90 %) in the Samunsam-Sematan coastal areas, which could  
25 potentially impact nearby coral reef habitats in this region. Study of the temporal TSS variation  
26 provides further evidence that monsoonal patterns drive the TSS release in these tropical water  
27 systems, with distinct and widespread TSS plume variations observed between the northeast and  
28 southwest monsoon periods. A map of relative TSS distribution anomalies revealed strong spatial TSS  
29 variations in the Samunsam-Sematan coastal areas, while 2010 recorded a major increase  
30 (approximately 100 %) and widespread TSS distribution with respect to the long-term mean.  
31 Furthermore, study of the contribution of river discharge to the TSS distribution showed a weak  
32 correlation across time at both the Lupar and Rajang river mouth points. The variability of TSS  
33 distribution across coastal river points was studied by investigating the variation of TSS pixels at three  
34 transect points, stretching from the river mouth into territorial and open water zones, for eight main  
35 rivers. The results showed a progressively decreasing pattern of nearly 50 % in relation to the distance  
36 from shore, with exceptions in the northeast regions of the study area. Essentially, our findings  
37 demonstrate that the TSS levels at the southwest coast of Sarawak are within local water quality  
38 standards, promoting various marine and socio-economic activities. This study presents the first  
39 observation of TSS distributions at Sarawak coastal systems with the application of remote sensing  
40 technologies, to enhance coastal sediment management strategies for the sustainable use of coastal  
41 waters and their resources.

42 **Keywords:** total suspended solids, band-ratio, monsoon, river discharge, Open Data Cube

43

44

45

## 46 1.0 Introduction

47 Total Suspended Solids (TSS) play an important role in the aquatic ecosystem as one of the primary  
48 water quality indicators of coastal and riverine systems (Alcântara et al., 2016; Cao et al., 2018; Chen  
49 et al., 2015a; González Vilas et al., 2011; Mao et al., 2012). For example, elevated concentrations of  
50 TSS in water have an adverse impact on fisheries and biodiversity of the aquatic ecosystem (Bilotta  
51 and Brazier, 2008; Chapman et al., 2017; Henley et al., 2000; Wilber and Clarke, 2001). Understanding  
52 the impacts of varying water quality in relation to TSS status has been one of the primary concerns  
53 with respect to a country's growing Blue Economy status and sustainable management of aquatic  
54 resources (Lee et al., 2020a; Sandifer et al., 2021; World Bank and United Nations Department of  
55 Economic and Social Affairs (UNDESA), 2017). With about 40 % of the world's population living within  
56 100 km of coastal areas (United Nations, 2017), and with more than 80 % of the population in Malaysia  
57 living within 50 km of the coast (Praveena et al., 2012), water quality monitoring and management  
58 efforts are important at both regional and global scale.

59 Studying TSS distribution can provide insights into the connections between land and ocean  
60 ecosystems (Howarth, 2008; Lemley et al., 2019; Lu et al., 2018). For instance, TSS dynamics allow us  
61 to understand the impacts of sediment transport and sediment plumes, particularly in areas  
62 experiencing large-scale deforestation, land conversion and damming of rivers (Chen et al., 2007;  
63 Espinoza Villar et al., 2013). Sarawak, Malaysian Borneo, experienced significant land use and land  
64 cover change activities over the past four decades, with widespread land conversion and deforestation  
65 for developments and large-scale plantation activities (Gaveau et al., 2016), as well as building of  
66 major road infrastructures, such as the Pan-Borneo highway, and hydroelectric dams (Alamgir et al.,  
67 2020). As a result, river and coastal systems may potentially drive large TSS loads into downstream  
68 systems and into the marine and open ocean waters.

69 Situated at the southern part of the South China Sea, the region of Sarawak, Malaysian  
70 Borneo, has a coastline of about 1035 km where mangrove forests are dominant (Long, 2014). The

71 coastal regions of Sarawak are rich with marine coastal biodiversity and coral reefs, which can be  
72 found at the northeast and southwest part of Sarawak (Praveena et al., 2012). While the coasts of  
73 Sarawak provide important socio-economic values to the local communities (Lee et al., 2020b), these  
74 coastal areas are potentially facing water quality degradation from TSS riverine outputs in response  
75 to land use and land cover change activities.

76 TSS concentrations are commonly measured through conventional laboratory-based methods  
77 to quantify TSS concentrations by field collection of water samples (Ling et al., 2016; Mohammad Razi  
78 et al., 2021; Soo et al., 2017; Soum et al., 2021; Tromboni et al., 2021; Zhang et al., 2013). Currently,  
79 real-time high-frequency TSS observations using modern optical and bio-sensor systems are also  
80 possible (Bhardwaj et al., 2015; Horsburgh et al., 2010). These sensors can be generally found onboard  
81 ship and buoy-based observation platforms. Yet, it remains a challenge to quantify TSS concentrations  
82 of large spatial coverage and high temporal frequency with these approaches.

83 Ocean colour remote sensing technologies represent an increasingly accessible and powerful  
84 tool to provide a synoptic view for short or long-term water quality studies at high temporal and spatial  
85 resolutions (Cherukuru et al., 2016a; Slonecker et al., 2016; Swain and Sahoo, 2017; Wang et al., 2017;  
86 Werdell et al., 2018). Remote sensing can help overcome several constraints of conventional intensive  
87 field campaigns such as: (i) costly field campaigns from boat rentals or cruise; (ii) time-consuming and  
88 inadequate manpower; and most importantly for this study, (iii) limited spatial and temporal field  
89 coverage. NASA's Moderate Resolution Imaging Spectroradiometer (MODIS)-Aqua  
90 (<https://modis.gsfc.nasa.gov/about/>) has a distinctive advantage with its daily revisit time, a spatial  
91 resolution of 250 – 1000 m, and a large collection of ocean colour data since 2002. Other sensors  
92 offering ocean colour measurement capabilities include Landsat-8, which, in comparison with MODIS-  
93 Aqua, has a 16-day revisit time and high spatial resolution of 30 m. Additionally, Sentinel 2-MSI (10 –  
94 60 m) and Sentinel 3-OLCI (300 m) missions provide global coverage of high resolution of ocean and  
95 land observations, with revisit time of 10-day and 2-day, respectively (European Space Agency, 2022a,

96 2022b). Despite Landsat 8 and Sentinel-2's powerful ability in capturing higher resolution images, the  
97 longer revisit interval may not be suitable for characterizing and studying large swath of coastal water  
98 bodies with high dynamics of various water constituents. While Sentinel 3-OLCI enhances in a shorter  
99 revisit time, this mission has a relatively smaller collection of ocean data stored, with the mission  
100 launched in 2016, in comparison to the MODIS-Aqua data collection.

101 Several MODIS-derived models have been developed for TSS retrievals (Chen et al., 2015b;  
102 Espinoza Villar et al., 2013; Jiang and Liu, 2011; Kim et al., 2017; Zhang et al., 2010b), including  
103 empirical, semi-analytical and machine-learning approaches (Balasubramanian et al., 2020; Jiang et  
104 al., 2021). However, the performance of these models proved to be unsatisfactory, with recorded low  
105  $r^2$  and high bias and mean absolute error (MAE) values when tested with in situ TSS datasets  
106 (Supplementary Materials, Table S1). Generally, optical water types are categorised based on the  
107 water reflectance signatures, which are influenced by varying optical water constituents such as the  
108 coloured dissolved organic matter, suspended sediment and phytoplankton presence in the water  
109 column (Aurin and Dierssen, 2012; Balasubramanian et al., 2020; Moore et al., 2009). While these  
110 global TSS remote sensing models address the need to improve TSS retrievals and to monitor global  
111 TSS trends in various water class types, they tend to underperform in more localised and regional  
112 studies (Mao et al., 2012; Ondrusek et al., 2012). The coastal waters of Borneo are well-mixed  
113 throughout the year and enriched with suspended material and dissolved organic matter (Müller et  
114 al., 2016). Various water quality studies of the river systems have been actively carried out to assess  
115 the dynamics of numerous water quality constituents in response to human activities, with TSS  
116 concentrations being one of the primary environmental concerns in this region (Ling et al., 2016;  
117 Müller-dum et al., 2019; Tawan et al., 2020). Although studies on the water quality of coastal systems  
118 in Borneo have gradually gained much attention (Cherukuru et al., 2021; Limciah et al., 2010; Martin et  
119 al., 2018; Soo et al., 2017), there is still much knowledge to gain on the understanding of how coastal  
120 waters in the region have been impacted by TSS loadings and transport over large spatial and temporal  
121 scales.

122 Here, in this paper, we present a new regional empirical TSS remote sensing model. While  
123 various remote sensing models have their own unique computational strengths, this study  
124 demonstrates the reliability of a band ratio TSS model when applied in optically complex waters. With  
125 the ongoing efforts to address and minimize water quality degradation in coastal systems, as outlined  
126 in the United Nation's Sustainability Development Goals no. 14, our study aims to apply the new  
127 empirical regional TSS remote sensing model to: (a) investigate the spatial and temporal variability in  
128 TSS, (b) identify hotspots of TSS distribution in the coastal waters of Sarawak, Malaysian Borneo, using  
129 a long time series of MODIS-Aqua data from year 2003 until 2019, and (c) study the varying monsoonal  
130 and river discharge patterns in relation to TSS distribution at the river mouths located within the study  
131 case area. With the growing accessibility of freely available satellite datasets, the application of Open  
132 Data Cube (ODC) platform provides an advanced tool to access scalable spatial imageries datasets and  
133 process time-series satellite data for earth observation studies (Open Data Cube, 2021). As such, this  
134 study implements the application of ODC platform which is further demonstrated in this study.

135

136

137

138

139

140

141

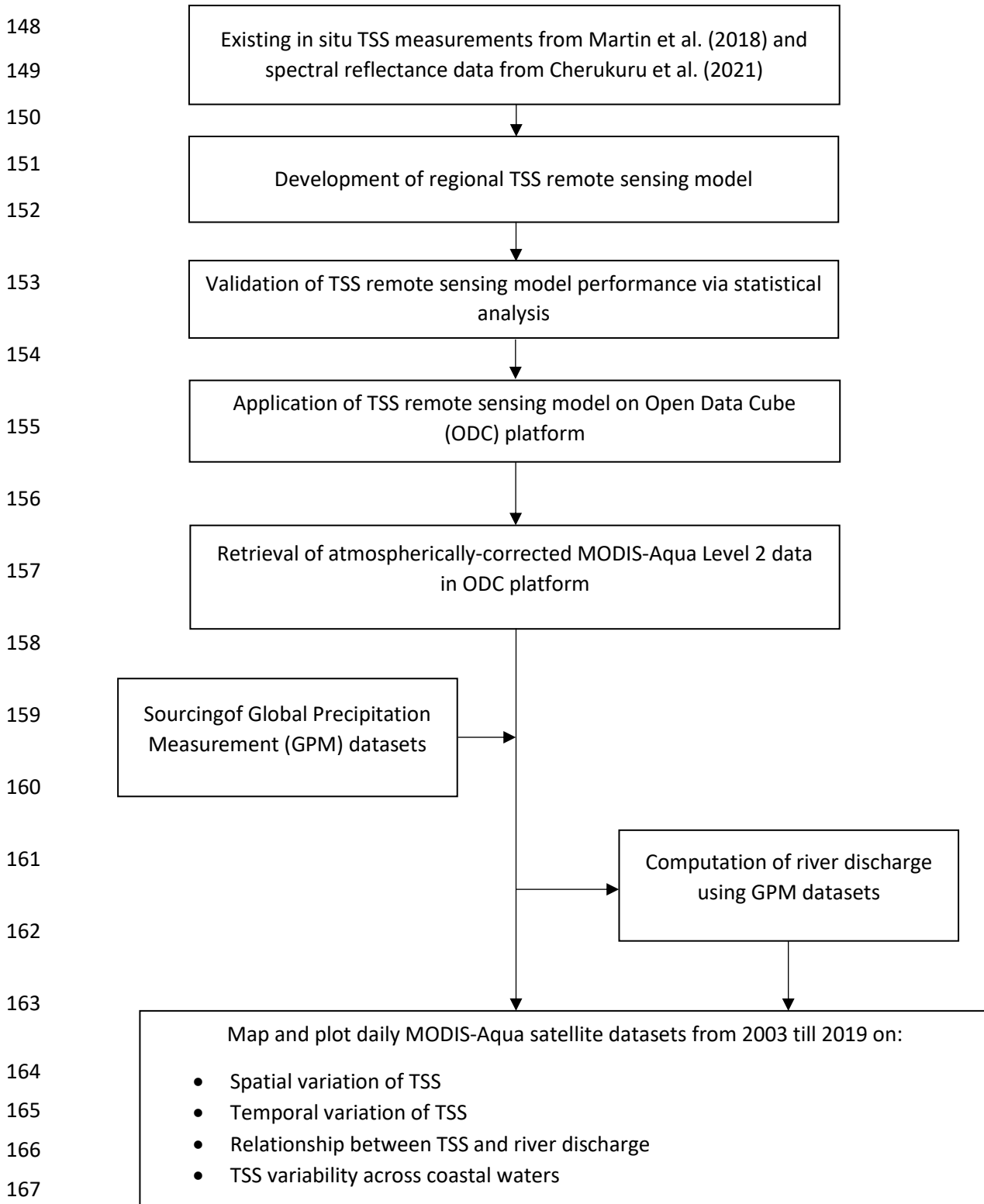
142

143

144

145 2.0 Methodologies

146 The figure below summarizes the processes carried out in this study. Spatial and temporal variation of  
147 TSS distribution was mapped using an atmospherically-corrected MODIS-Aqua Level 2 product.



168 Fig. 1: Flowchart summarizing the processes of developing a regional TSS remote sensing model and applying it to analyse  
169 the spatial and temporal variation of TSS over the study region, using MODIS-Aqua data from year 2003 until 2019. Long-  
170 term MODIS-Aqua datasets were analysed and mapped on an Open Data Cube (ODC) platform with implementation of robust  
171 Python libraries and packages.

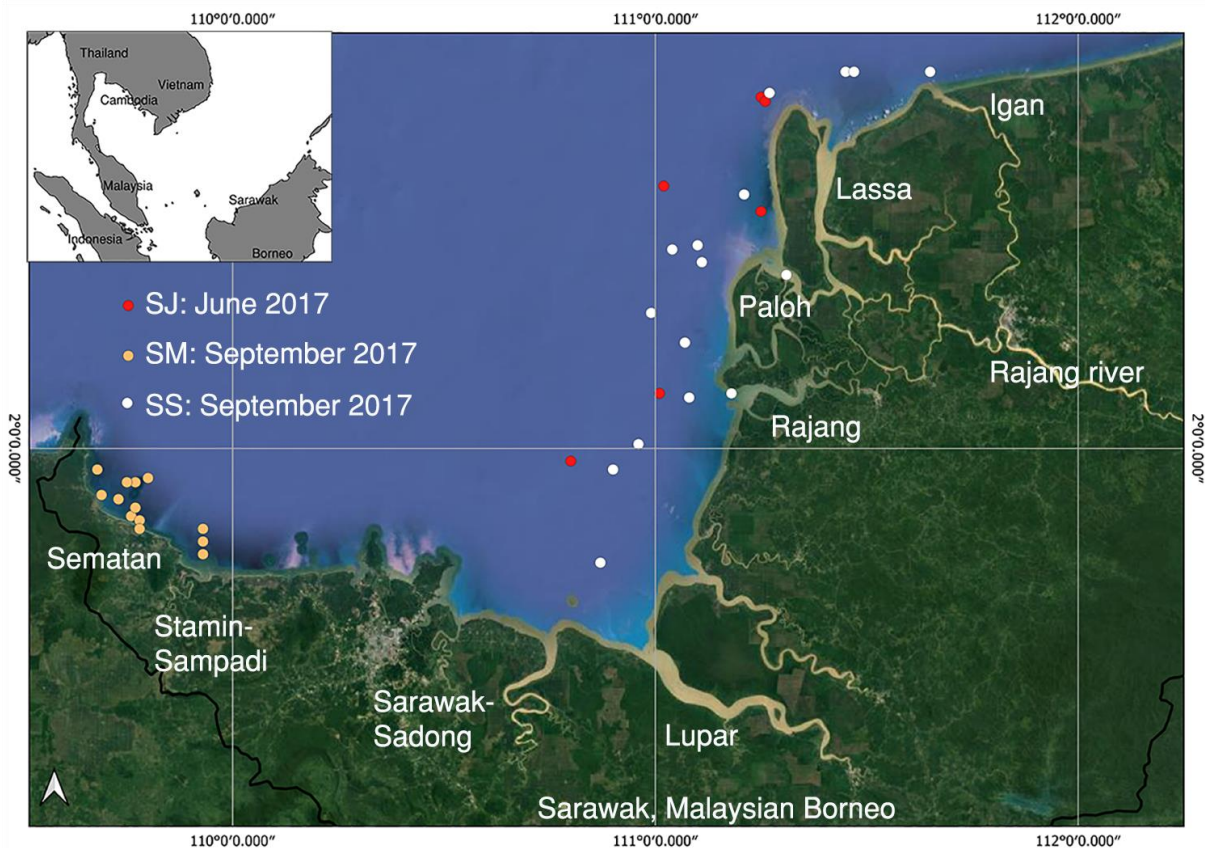
172

## 173 2.1 Area of study

174 Our study focuses on the southwestern coast of Sarawak (between 1.9° N, 109.65° E and 2.8° N, 111.5°  
175 E) in Malaysia, which sits at the northwest part of the Borneo Island. Generally, the island of Borneo  
176 (between 3.01° S, 112.18° E and 6.45° N, 117.04° E) contains rich tropical rainforests and biodiversity  
177 on the lands of Sarawak and Sabah (Malaysia), Brunei, and Indonesia. Typically, Sarawak is a tropical  
178 climate region, recording an average ambient temperature of 27.8 °C (variation of 1.8 °C) throughout  
179 the year. It records high precipitation with an average of 4116.7 mm/yr in Kuching (1.5535° N,  
180 110.3593° E), the capital city of Sarawak. Yearly, it experiences both a dry and wet season, which is  
181 influenced by: (i) the southwestern monsoon (May to September) and (ii) the northeastern monsoon  
182 (November to March). Rivers in Sarawak are connected to the South China Sea and flow through  
183 various plantation types, such as palm oil, rubber and sago (Davies et al., 2010).

184 In this study, the southwestern part of Sarawak's coastal regions (Fig. 2), (between 1.9° N, 109.65° E  
185 and 2.8° N, 111.5° E) was studied, which comprises several major rivers (e.g. Lupar, Sebuyau,  
186 Sematan), as well as the Rajang River, the longest river in Malaysia. Rajang river basin consists of a  
187 tidal river channel which splits into a northwest (Igan, Lassa and Paloh) and a southwest (Rajang,  
188 Belawai) Rajang river delta (Staub et al., 2000). The Rajang river basin drains a dominant area  
189 (>50,000km<sup>2</sup>) of sedimentary rocks (Milliman and Farnsworth, 2013; Staub et al., 2000) extending  
190 from Belaga to Sibu, with major peatland areas converted into palm oil plantations (Gaveau et al.,  
191 2016) as its river flows into the South China Sea (Milliman and Farnsworth, 2013). Major settlements  
192 along the Rajang river comprise of Kapit and Kanowit town areas, as well as Sibu city, with a total  
193 population size of about 388,000 inhabitants (Department of Statistics, 2020). Lupar and Saribas  
194 rivers, respectively, comprise a catchment area size of approximately 6500 and 1900 km<sup>2</sup> (Lehner et  
195 al., 2006). Situated at the southwest side of the Rajang catchment, Lupar and Saribas rivers surround

196 the Maludam National Park, which is Sarawak's remaining biggest single patch of peat swamp forest  
197 (Sarawak Forestry Corporation, 2022). Adjacent to Lupar river mouth is the Sadong river, with an  
198 approximate catchment area size of 3500 km<sup>2</sup> (Kuok et al., 2018). Sadong river is about 150 km long  
199 and flows through palm oil plantations (Staub and Esterle, 1993). These river systems are associated  
200 with increasing land use activities and land cover changes in this region, which essentially transport  
201 and connect various biogeochemical water components to the coastal systems of Sarawak.



202  
203 Fig. 2: Map of the study area (© Google Maps), located in the southwestern part of Sarawak, Malaysia (inset). Indicators  
204 show the location of sampling sites used during field expeditions carried out in June and September 2017.

## 205 2.2 In situ TSS measurements

206 TSS measurements were taken from Martin et al. (2018). A total of 35 coastal sites were studied and  
207 are denoted SJ, SS, and SM (see: Table 1 & Fig. 2). These water samples were collected in the month  
208 of June (SJ region) and September (SS and SM regions) in 2017. Water samples were filtered, and



209 filters were dried and ashed prior to the weighing process. Full details of the water sampling and TSS  
210 analysis are available in Martin et al. (2018).

### 211 2.3 Development, calibration and validation of TSS model

212 In situ remote sensing reflectance spectral data,  $R_{rs}(\lambda)$ , along with 35 measured TSS values, were used  
213 to develop a new remote sensing TSS empirical model for MODIS-Aqua for this case study. Field  
214 measurements of SM, SJ & SS datasets, as shown in Table 1, were used to calibrate the MODIS-Aqua  
215 TSS remote sensing model.

216 For the in situ remote sensing reflectance,  $R_{rs}(\lambda)$  readings, a TriOS-RAMSES spectral imaging  
217 radiometer was used to measure downwelling irradiance,  $E_d(\lambda)$ , and upwelling radiance,  $L_u(\lambda)$ , with  
218 measurement protocols from Mueller et al. (2002). These measurements were recorded under stable  
219 sky and sea conditions during the day (10AM to 4PM) with high solar elevation angles.

220 Measurements of reflectance,  $R_{rs}(\lambda)$ , were recorded concurrently with the collection of water samples  
221 (as described in Section 2.2) and were recorded at wavelength ranging from 280 to 950 nm, which  
222 covers the spectrum of ultraviolet, visible and near-infrared bands . These measurements were  
223 recorded on a float to capture  $L_u(0-, \lambda)$  and  $E_d(0+, \lambda)$ , where 0- and 0+ refer to below-surface and  
224 above-surface, respectively.

225 Remote sensing reflectance,  $R_{rs}(\lambda)$ , was computed as follows with reference to Mueller et al. (2002):

$$R_{rs}(\lambda, 0+) = \frac{1 - p}{n^2} \times \frac{L_u(0-, \lambda)}{E_d(0+, \lambda)} \quad (1)$$

226 where  $p = 0.021$  refers to the Fresnel reflectance and  $n = 1.34$  is the refractive index of water. Full  
227 details of this methodology can be found at Cherukuru et al. (2021).

#### 228 2.3.1 Calibration of empirical model and application to MODIS-Aqua

229 With the intention to apply a regional TSS remote sensing model to MODIS-Aqua data, a total of 35 in  
230 situ spectral data of different TSS datasets , which were collected in coastal conditions (salinity > 15

231 PSU), were convolved with MODIS-Aqua spectral response function values (Pahlevan et al., 2012) at  
232 each centre wavelength of individual band channels (NASA official, 2022). MODIS-Aqua offers visible  
233 bands of violet/blue (412, 443, 469, and 488 nm), green (531, 547, and 555 nm), red (645, 667, and  
234 678 nm) and near-infrared wavelengths (748, 859 and 869 nm) for remote sensing of coastal waters  
235 (NASA official, 2022). The in situ spectra data were resampled to MODIS-Aqua's central spectral bands  
236 based on the aforementioned information. Measurements of in situ spectral data enhance the  
237 understanding of bio-optical water characteristics of a localised region, and increase the sensitivity of  
238 radiometric measurements without atmospheric interferences, while subject to the radiometer's  
239 calibration condition (Brezonik et al., 2015; Cui et al., 2010; Dorji and Fearn, 2017; Slonecker et al.,  
240 2016).

241 In this study, retrieval of water constituents was established using spectral band ratio combinations  
242 which have proven to be a straightforward, yet reliable method for estimating water constituents in  
243 optically turbid waters (Ahn and Shanmugam, 2007; Cao et al., 2018; Lavigne et al., 2021; Morel and  
244 Gentili, 2009; Neil et al., 2019; Siswanto et al., 2011). Band ratio models help to offset signal noise,  
245 such as the effects of the atmospheree and irradiance of spectral reflectance to a certain degree  
246 (Cherukuru et al., 2016b; Ha et al., 2017; Hu et al., 2012; Liu et al., 2019).

247 A variety of models using single bands, as well as a combination of MODIS-Aqua's Blue, Green & Red  
248 bands (412nm, 440nm, 488nm, 532nm, 555nm & 660nm) were calibrated using field measurements  
249 as the dependent variable. The calibration process was tested out using various model functions,  
250 including linear, power, exponential, and logarithmic functions. The best empirical TSS retrieval model  
251 was fitted by means of a regression between the in situ TSS data and in situ radiometer values, and  
252 can be expressed as follows:

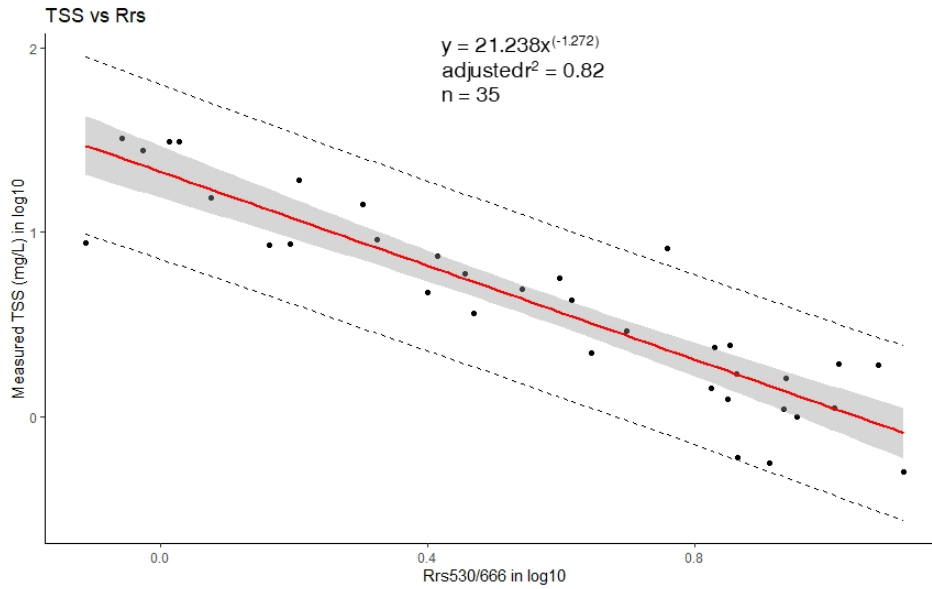
$$253 \quad \text{TSS} = 21.238[\text{Rrs}(530)/\text{Rrs}(666)]^{-1.272} \quad (2)$$

254 This power function model resulted in a coefficient of determination ( $R^2$ ) of 0.82 (Fig. 3).

255 Table 1: Summary statistics of TSS values collected at areas SJ, SS, and SM located within coastal regions in this study, with a  
256 total of 35 datasets recorded.

Coastal Area	Minimum	Maximum	Mean	S.D.	C.V.	n
SJ	1.1	19.24	6.89	6.62	96.09	6
SS	0.56	32.1	12.50	11.43	91.45	16
SM	0.5	8.14	2.59	2.70	104.53	13

257



258

259 Fig. 3: Empirical relationship of TSS retrieval between in situ Rrs(530)/Rrs(666) bands ratio and measured TSS  
 260 concentration (mg/L), as established via a power law function. Upper and lower dashed lines indicate the 95 % prediction  
 261 interval of the regression.

262 2.3.2 Performance assessment and validation of MODIS-Aqua empirical model

263 An assessment of the performance error of the newly developed TSS model was carried out as per  
 264 Seegers et al. (2018)'s recommendation for interpreting ocean colour models. These performance  
 265 metrics used here include the bias, Mean Absolute Error (MAE), Root Mean Squared Error (RMSE),  
 266 coefficient of variation (CV), as well as the coefficient determination,  $r^2$ , based on the following  
 267 calculations:

268 
$$\text{Bias} = 10^{\wedge} \left[ \frac{\sum_{i=1}^n \log_{10}(Mi) - \log_{10}(Oi)}{n} \right] \quad (3)$$

269 
$$\text{MAE} = 10^{\wedge} \left[ \frac{\sum_{i=0}^n | \log_{10}(Mi) - \log_{10}(Oi) |}{n} \right] \quad (4)$$

270 
$$\text{RMSE} = \sqrt{\frac{\sum_{i=1}^n (\log_{10}(Mi) - \log_{10}(Oi))^2}{n}} \quad (5)$$

271 
$$CV = \frac{\sigma}{\mu} \times 100\% \quad (6)$$

272 where M represents the modelled TSS values, n is the number of samples, and O represents the  
 273 observed TSS measurements, while  $\sigma$  refers to standard deviation and  $\mu$  represents the mean value.

274 Equations (3), (4) and (5) use a log10-transform of the data as the range of TSS values can span several  
 275 orders of magnitude. As such, an application of the log-transformation prior to error metric calculation  
 276 allows us to account for uncertainties that are proportional to the concentration values  
 277 (Balasubramanian et al., 2020; Seegers et al., 2018).

278 Table 2: Calibration and accuracy assessment of the newly derived MODIS-Aqua models in this study for TSS estimations  
 279 tested using various model functions. Calculation for bias, MAE and RMSE use a log-transformation of the data prior to  
 280 calculation of error metric measurements, as adapted from Seegers et al. (2018) and Balasubramanian et al. (2020). Band  
 281 ratio Rrs(530)/Rrs(666) is established as function x. The power function model is selected based on low performance metric  
 282 values.

Model	Function	Bias	MAE	RMSE	CV (%)	R
Power	TSS = 21.238x <sup>-1.272</sup>	0.9999	1.4732	0.2161	4.74	0.84
Linear	TSS = -1.8193x + 16.928	1.4463	1.8549	6.7174	20.699	0.6854
Exponential	TSS = 17.784e <sup>-0.296x</sup>	1.0791	1.4906	6.3088	3.8920	0.8154
Logarithmic	-8.872ln(x)+19.383	1.1336	1.6177	5.3735	-17.056	0.8128

283  
 284 An evaluation of the model was performed using a k-fold cross validation technique (Refaeilzadeh et  
 285 al., 2020) given the small size of the TSS dataset used in this study (Table 2). A selection of k = 7 was  
 286 assigned to split the datasets into k groups with an equal number of data points.

287 Table 2: Assessment of fitting error for the proposed TSS model, using k-fold cross validation.

Parameter	k-fold (n)	R2	RMSE	MAE
TSS	7	0.85	0.2159	0.1747

288

289 While these results point to low error levels achieved by the proposed regional TSS retrieval model  
290 (Table2), caution should be used when applying it to various water types. Water type classification has  
291 been thoroughly described by Balasubramanian et al. (2020) where waters are classed into Type I  
292 (Blue-Green waters), Type II (Green waters), and Type III (Brown waters). Essentially, the Green-to-  
293 Red band ratio is optimised with these datasets corresponding to sediment-dominated and yellow-  
294 substance loaded water conditions. As highlighted by Morel & Belanger (2006), waters of this type do  
295 not have the same spectral characteristics as phytoplankton-rich waters (also known as Case 1  
296 waters). In addition to the impact on water clarity, sediment particles (often red-brownish coloured)  
297 also tend to enhance the backscattering and absorption properties, especially at shorter wavelengths  
298 (Babin et al., 2003), while the additional presence of coloured dissolved matter (yellow substance)  
299 leads to strong absorption properties at short wavelengths. As the TSS retrieval model was developed  
300 from samples taken in waters that are bio-optically rich in suspended solids and dissolved organic  
301 matter, an application of this TSS model needs to be done cautiously when applying to other water  
302 types, particularly those with large concentration of phytoplankton.

#### 303 2.4 Application of TSS retrieval model

304 Daily MODIS-Aqua satellite data from year 2003 to 2019 (total of 6192 individual time slices) were  
305 studied with a 2°x 2° spatial resolution (longitude: 109.38, 112.0; latitude: 1.22, 3.35) which covers  
306 the southwestern coastal region of Sarawak and southern part of the South China Sea.  
307 Atmospherically corrected MODIS-Aqua level 2 reflectance data (Bailey et al., 2010; NASA Official,  
308 n.d.) were retrieved for the application of the TSS model proposed in this study. Negative remote  
309 sensing reflectance values, possibly due to failure of atmospheric correction, were filtered out before  
310 applying the retrieval model, as expressed in Eq. (2), to map the spatial and temporal distribution of  
311 TSS estimates. In addition, averaging of spatial and temporal TSS variation maps in this study was  
312 carried out by filtering TSS values with fewer than 10 valid data points over the whole time series,

313 along with application of sigma clipping operation (refer to:  
314 [https://docs.astropy.org/en/stable/api/astropy.stats.sigma\\_clip.html](https://docs.astropy.org/en/stable/api/astropy.stats.sigma_clip.html)).

#### 315 2.4.1 Open Data Cube

316 In this study, the analysis of remote sensing data over large spatial extents and at high temporal  
317 resolution was carried out using robust Python libraries and packages run on an Open Data Cube (ODC)  
318 platform. Open Data Cube is an open-source advancement in computing technologies and data  
319 architectures which addresses the growing volume of freely available Earth Observation (EO) satellite  
320 products (Giuliani et al., 2020; Killough, 2019). ODC provides a collection of software which index,  
321 manage, and process large EO datasets such as satellite products from the MODIS, Landsat and  
322 Sentinel missions (Gomes et al., 2021). These satellite datasets are structured in a multi-dimensional  
323 array format, and provide layers of information across latitude and longitude (Open Data Cube, 2021).  
324 Leveraging the growing availability of Analysis Ready Data (ARD), and with support from the  
325 Committee of Earth Observation Satellites (CEOS) (Killough, 2019), the ODC concept has been  
326 deployed in many countries across the world. These existing deployments include Digital Earth Africa  
327 (<https://www.digitalearthafrika.org/>), Digital Earth Australia (DEA) (<https://www.dea.ga.gov.au/>),  
328 Vietnam Open Data Cube (<http://datacube.vn/>), and Brazil Data Cube ([https://github.com/brazil-data-](https://github.com/brazil-data-cube)  
329 [cube](https://github.com/brazil-data-cube)), which provide various time-series datasets of the changing landscape and water content in  
330 these specific regions (Giuliani et al., 2020; Gomes et al., 2021; Killough, 2019; Lewis et al., 2017). The  
331 ecosystem and architecture of ODC is well explained at [opendatacube.org](https://opendatacube.org). The codes and tools used  
332 in this application drew upon the information provided in various DEA notebooks (Krause et al. (2021),  
333 which can be found at <https://github.com/GeoscienceAustralia/dea-notebooks/>.

#### 334 2.5 Precipitation data and computation of river discharge

335 Monthly precipitation values (mm) over the Lupar and Rajang basins were extracted from the Global  
336 Precipitation Measurement (GPM) Level 3 IMERG satellite datasets  
337 (<https://gpm.nasa.gov/data/imerg>) in order to assess the influence of precipitation in each river basin

338 in relation to TSS concentration at the corresponding river mouth (Supplementary Materails, Fig. S4 –  
339 7).

340 Derivation of river discharge ( $m^3/s$ ) was computed using total precipitation estimates (mm) over each  
341 river basin, and multiplied by a surface discharge runoff factor for the studied region (Sim et al., 2020).  
342 The surface runoff was estimated to be 60 % of total precipitation (Staub et al., 2000; Whitmore,  
343 1984). In this study, the Rajang river basin, as well as the combined basins of the Lupar, Sadong, and  
344 Saribas rivers (hereafter referred to as the Lupar basin), were studied for their river discharge rates in  
345 relation to TSS release.

### 346 3.0 Results & Discussion

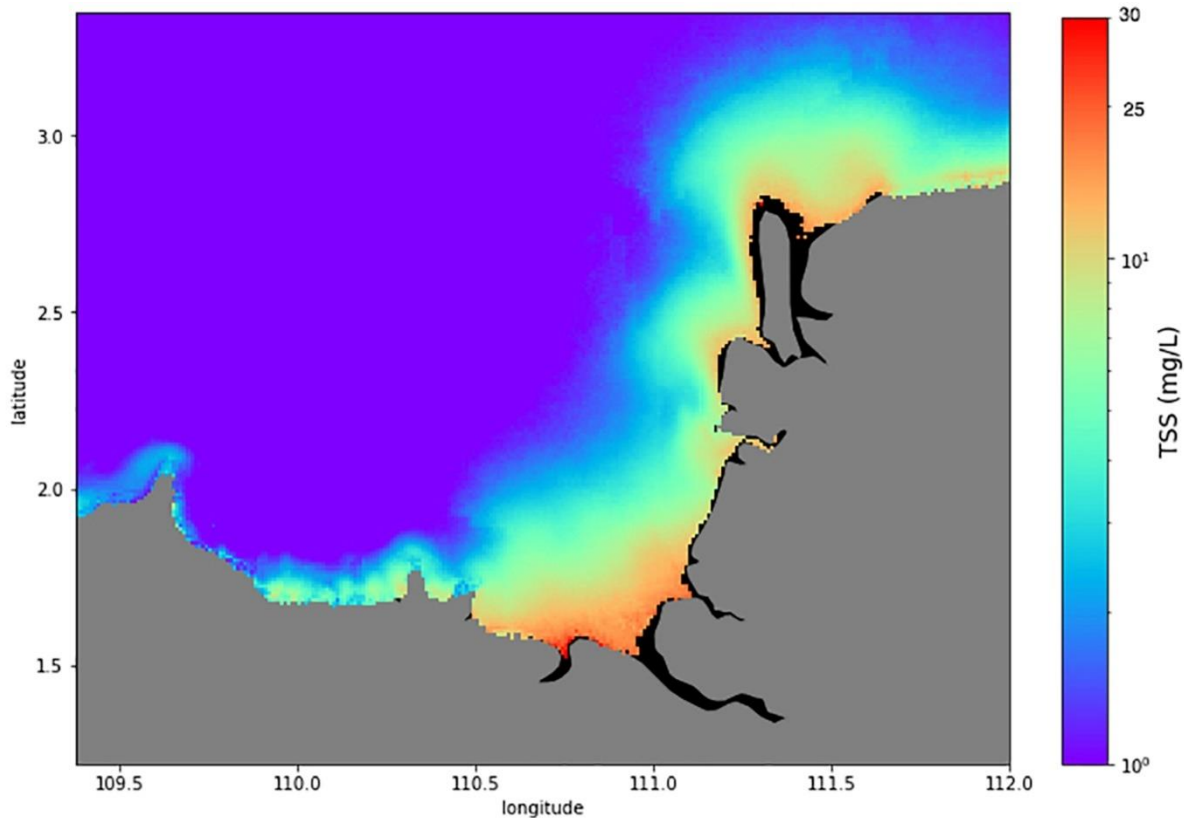
#### 347 3.1 Spatial variation of TSS distribution

348 Changes in TSS distribution occur across space and time. The regional TSS remote sensing model  
349 calibrated in this study was applied to the time series of MODIS-Aqua data to study the variability of  
350 spatial TSS distribution and identify potential hotspot areas susceptible to TSS water quality  
351 degradation. The map of average TSS for the Sarawak region was generated (Eq. 2) by averaging all  
352 the daily MODIS-Aqua TSS images (2003 to 2019) and is presented in Fig. 4. The results show that the  
353 waters in the northeast region of the study area, stretching from the Sadong river to the Rajang/Igan  
354 river have seen sustained levels of TSS over the 17 years considered in this study.

355 The temporally averaged spatial distribution map (Fig. 4) shows TSS concentrations in the range of 15  
356 – 20 mg/L near the river mouth areas, with widespread TSS plumes extending into the South China  
357 Sea (Fig. 5). Based on the Malaysia Marine Water Quality Criteria and Standard (Supplementary  
358 Materials, Table S2) (Department of Environment, 2019), these coastal waters fall under Class 1 in  
359 relation to their TSS (mg/L) status. This classification indicates that these coastal waters support and  
360 preserve marine life in this local region. Yet, several studies have expressed concerns regarding high  
361 TSS loadings in riverine waters owing to the impacts of various land use and land cover changes (LULC)

362 (Ling et al., 2016; Tawan et al., 2020). Among these, the Rajang river has been highlighted to be heavily  
363 impacted by various LULC activities such as large-scale deforestation and construction of hydropower  
364 dams (Alamgir et al., 2020). In situ water quality studies by Ling et al. (2016) reported on high TSS  
365 estimates at one of the upstream tributaries of Rajang river, the Baleh river, with TSS readings up to  
366 approximately 100 mg/L. Another study by Tawan et al. (2020) reported a significant TSS release  
367 reaching to 940,000 mg per day during wet seasons, with maximum TSS concentrations of 1700 mg/L  
368 in the upstream tributaries of the Rajang river, particularly at the Baleh and Pelagus rivers. The  
369 majority of the upstream tributary rivers were categorised as Class II (during dry season) and Class III  
370 (during wet season) waters according to the National Water Quality Index (Supplementary Materials,  
371 Table S3) (Department of Environment, 2014), due to increased soil erosion from surrounding LULC  
372 activities (Tawan et al., 2020). These local in situ findings provide valuable insights on point source TSS  
373 estimates in these LULC change regions. Coupled with our spatial map of average TSS captured by  
374 remote sensing technologies, our findings seem to suggest that a large portion of TSS loadings from  
375 inland and upstream rivers would have settled and deposited in these river channels and were not  
376 completely discharged outwards into the coastal areas, which would have caused major water quality  
377 degradation in the corresponding coastal systems.





378

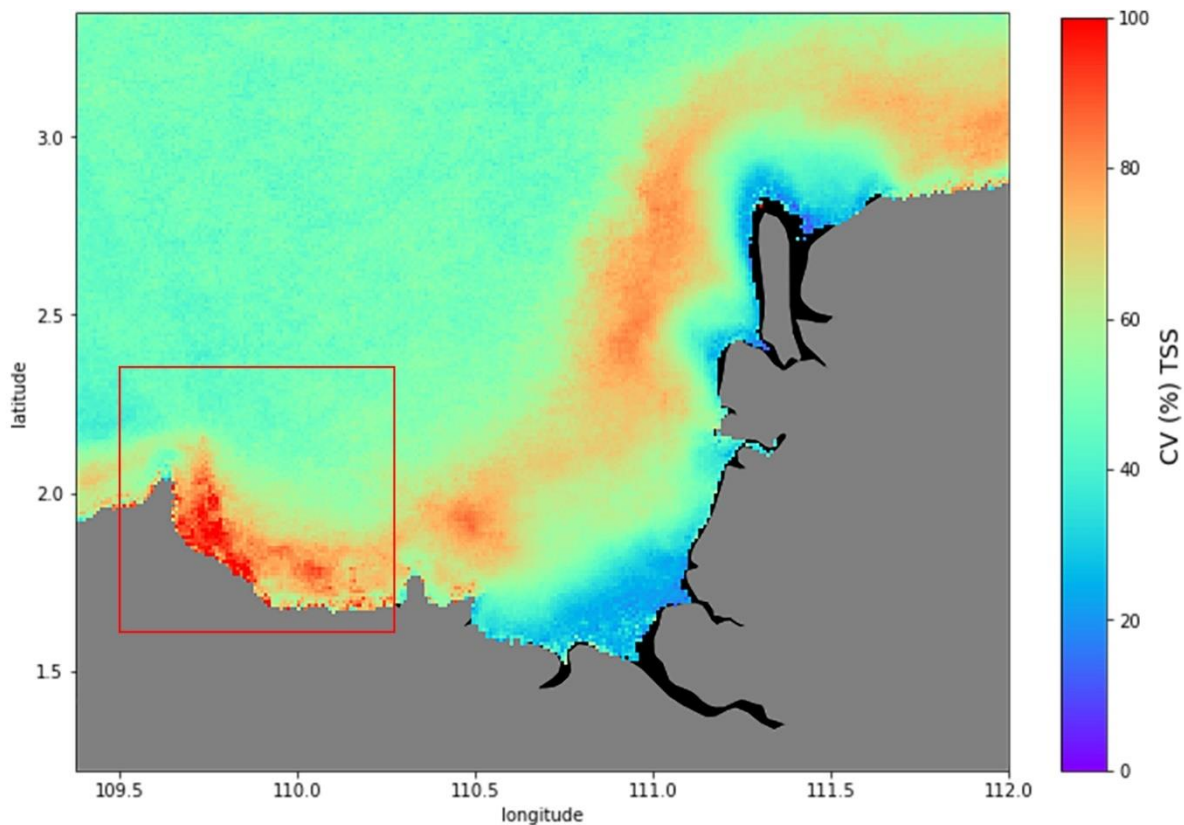
379 Fig. 4: Temporally averaged 2°x 2° map of TSS distribution (on a log scale) across the time dimension for each pixel.

380 Historical patterns of TSS concentration were assessed by comparing annual maps of average TSS  
 381 distribution (Supplementary Materials; Fig. S1), as well as time series of TSS estimates at the Lupar  
 382 and Rajang river mouths (Supplementary materials; Fig. S2). From our findings, the annual TSS maps  
 383 further support the observation where TSS release was evident at Lupar and Rajang/Igan river mouths  
 384 from 2003 till 2019, which points to Class I of local water quality standards in relation to TSS (mg/L)  
 385 status. This was found to consistently occur every year. Furthermore, the TSS trend study showed that  
 386 both the Lupar and Rajang river mouth points have a gradual increase of TSS concentration over the  
 387 17 years (Supplementary materials; Fig. S2). This increasing trend was, however, not statistically  
 388 significant ( $p = 0.43$  for Lupar, and  $p = 0.15$  for Rajang).

389 Moreover, a map of the TSS coefficient of variation (CV) was computed to identify areas with a high  
 390 degree of relative TSS variation over time (Fig. 5). Here again, the map of CV (%) was produced by  
 391 aggregation of the daily MODIS-Aqua images (6192 time steps) from 2003 until 2019. Figure 5 shows

392 that the Samunsam-Sematan coastal region (as highlighted by the red box) exhibits an increased level  
393 of TSS distribution variability, with a recorded CV of more than 90 %.

394 The Samunsam-Sematan coastal region contains near-pristine mangrove forests which are sheltered  
395 from major LULC activities, as compared to other studied sites. Samunsam-Sematan is also well-known  
396 locally as a recreational hotspot with coral reefs and various national parks (Sarawak Tourism Board,  
397 2021). Data from the Centre for International Forestry Research (CIFOR) Forrest Carbon database  
398 (CIFOR, n.d.) revealed that there was more than double the amount of total forest loss (approx. 5,000  
399 Ha) recorded in Lundu, a nearby township in the Sematan area in 2011 as compared to the previous  
400 years. Deforestation activities, regardless of their scale, can inevitably promote sediment loss and soil  
401 leaching into the nearby river systems (Yang et al., 2002). Important information regarding the  
402 variability in water quality (as shown in Fig. 5) can provide support to local authorities and relevant  
403 agencies in order to identify vulnerable areas that need to be monitored closely, such as the Lundu-  
404 Sematan region in this case. The CV map thus offers interesting insights into how TSS distribution can  
405 vary across large spatial areas, which can ultimately impact local socio-economic activities in this  
406 region (Lee et al., 2020b).



407

408 Fig. 5: Map of CV (%) calculated from the daily time series of MODIS-Aqua satellite images from 2003 until 2019.

### 409 3.2 Temporal variation of TSS distribution

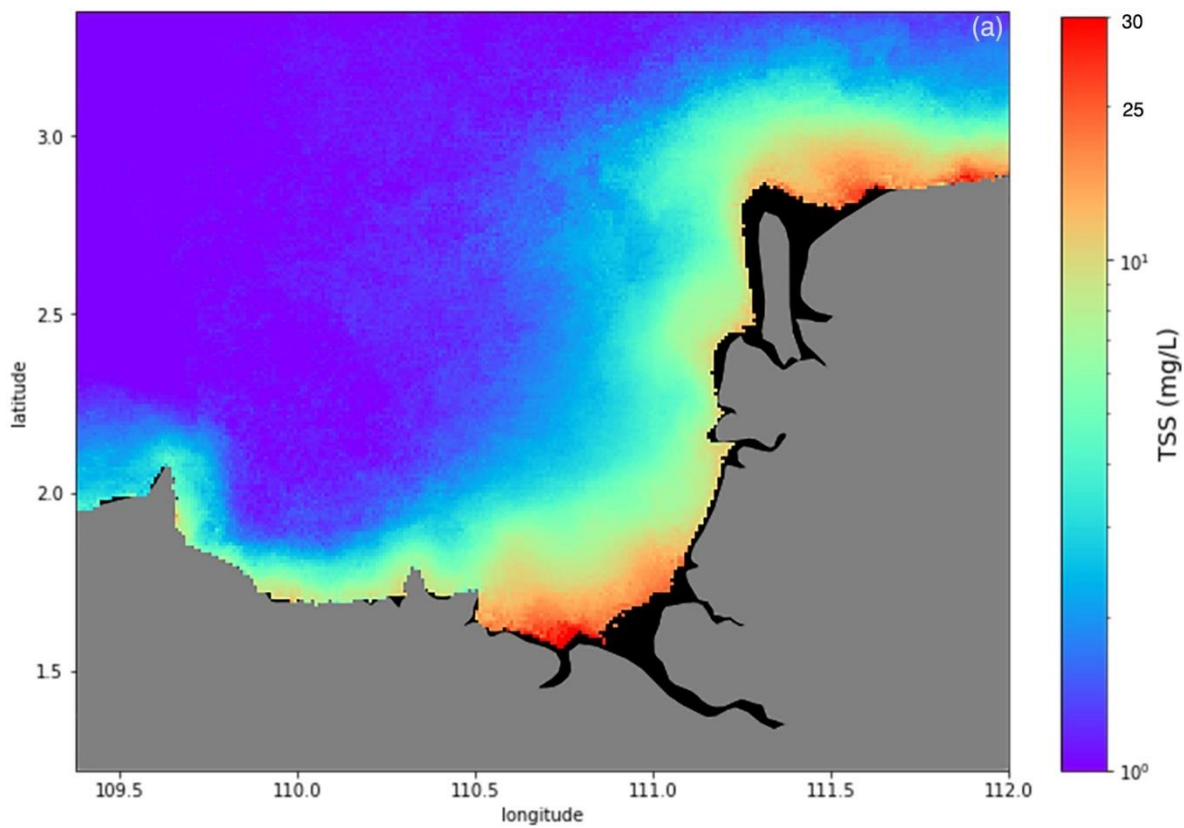
410 On a temporal scale, the northeast (NE) monsoon period shows a distinct difference in the widespread  
 411 intensity of TSS distribution as compared to the southwest (SW) monsoon period, along the Sarawak  
 412 coastline over the 17 years of the considered time series (Fig. 6). Mapping of temporal variations  
 413 between monsoons using time-series MODIS-Aqua datasets can provide an improved understanding  
 414 on the intensity of monsoonal patterns in driving the TSS distribution in this region. As shown in Figure  
 415 6, TSS release can be seen to extend further into the open ocean South China Sea region during the  
 416 NE monsoon periods (Fig. 6a) in comparison to the SW monsoon periods (Fig. 6b).

417 In addition, the differences in TSS release between the NE and SW monsoons  $((NE-SW)/NE \times 100)$  were  
 418 mapped as shown in Fig. 6c. Widespread TSS plumes are detected at Lundu/Sematan region ( $>80\%$   
 419 relative difference in TSS concentration) on the southwest side of the study area, while substantial  
 420 TSS plumes are observed in front of the Igan river channel, with more than  $50\%$  relative difference in

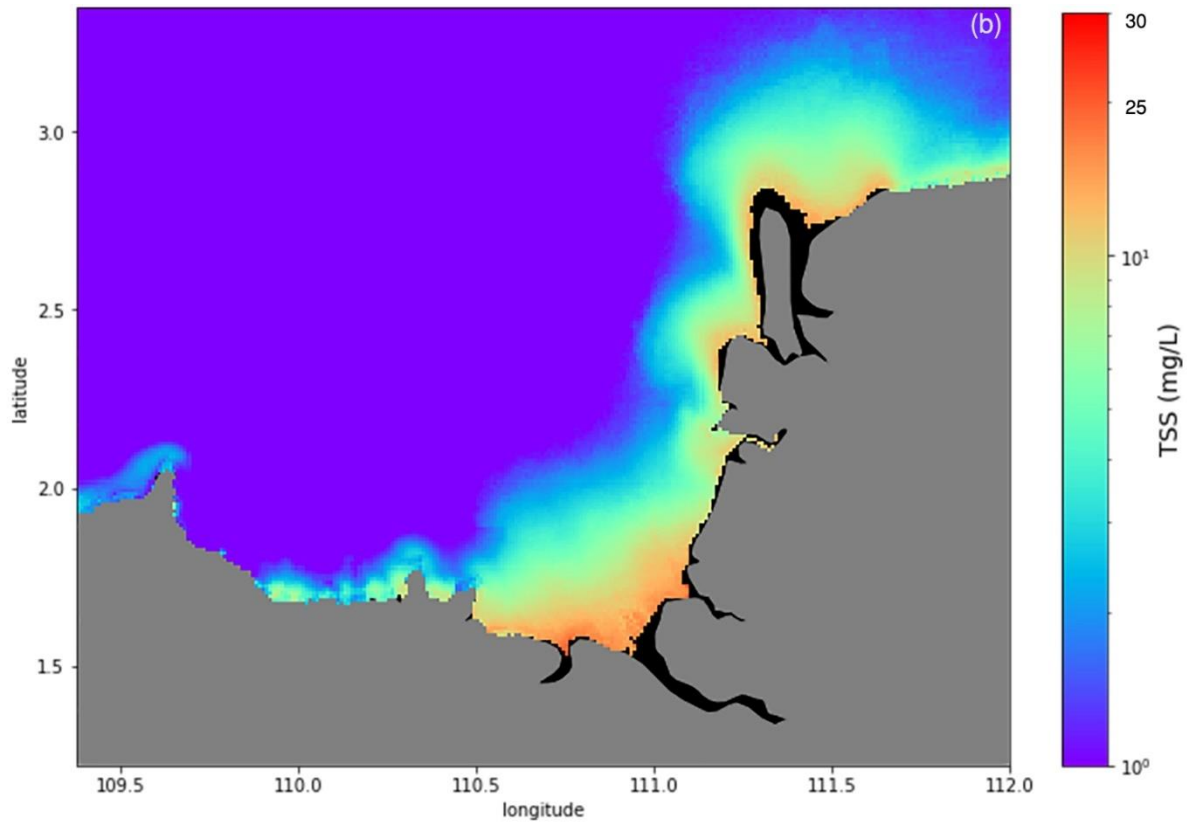
421 TSS concentration in comparison to SW monsoon periods. Sadong coastal area is observed to receive  
422 considerable TSS loadings (> 30%) during NE monsoon periods.

423 These coastal areas would thus be more likely to be impacted by the TSS release during the NE  
424 monsoon periods. These findings further strengthen the evidence that tropical rivers are majorly  
425 impacted by climatic variability such as monsoonal patterns, as highlighted in a study at Baleh river in  
426 Sarawak (Chong et al., 2021). This suggests that monsoon rains, which typically last for several months,  
427 play an integral role in driving the discharge of TSS in tropical rivers.

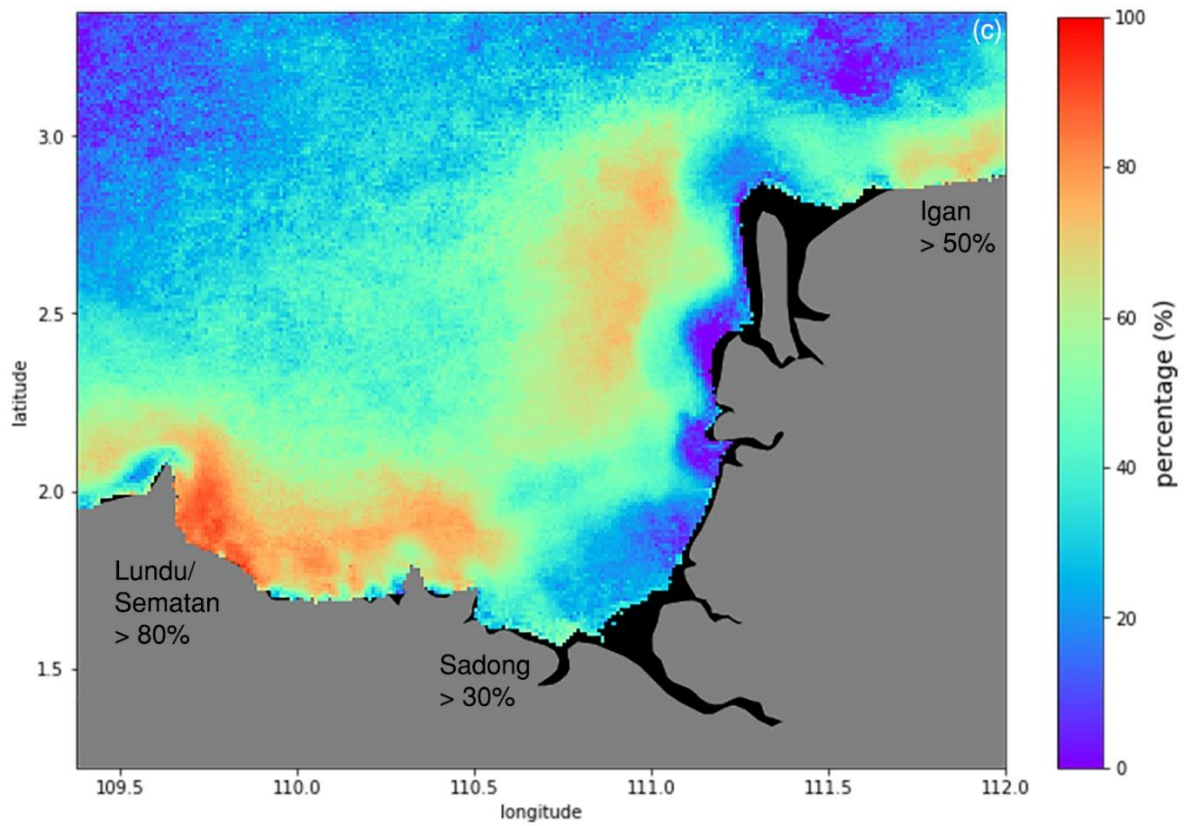
428



429



430



431

432 Fig. 6: Long-term average of TSS estimates (mg/L) during the Northeast monsoon (a), and the Southwest monsoon (b). The

433 map of TSS difference between the Northeast and Southwest monsoon periods, computed in relative percentage (%), is  
434 shown in (c).

435 Several climatic studies in the Borneo region highlighted 2009 as a year with extreme rainfall events  
436 which caused major floods in Sarawak (Dindang et al., 2011; Sa'adi et al., 2017), while drought events  
437 were reported in 2014 (Bong and Richard, 2020). Hence, in this study, TSS dynamics for the Lupar and  
438 Rajang rivers were studied by assessing the variation of TSS values at selected pixels in relation to  
439 monsoonal rainfall patterns in 2009 and 2014 (Supplementary Materials; Fig. S3).

440 Generally, the results show fluctuations of TSS concentrations across the NE and SW monsoon periods  
441 in relation to precipitation values (Fig. 7a – d). Based on Fig. 7a, monthly precipitation values recorded  
442 for the Lupar river basin in 2009 showed a clear decreasing trend from the NE monsoon period (wet  
443 season) to the SW monsoon period (dry season), while gradually increasing approaching the year end's  
444 NE monsoonal period. A similar precipitation pattern was observed for the Rajang river basin during  
445 the same year (Fig. 7c).

446 However, these results also show that the TSS distribution (mg/L) at the Lupar river mouth seems to  
447 show no distinct trend of decreasing TSS concentration estimates during the SW monsoon period in  
448 year 2009 (Fig. 7a) in relation to its precipitation values. Additionally, a sharp rise of TSS release can  
449 be seen in the month of May (beginning of SW monsoon period), with a near equivalent intensity of  
450 TSS release during the NE monsoon period. This observation may potentially be caused by the lag  
451 between the time of rainfall events occurring during NE monsoon periods and TSS release entering  
452 the coastal river regions. A similar observation was described by Sun et al. (2017a) suggesting that  
453 riverine outputs could take several days, and even up to one month to reach the coastal river points.  
454 Considering the occurrence of extreme rainfall events in 2009, our findings are in agreement with  
455 these processes as TSS concentrations generally exhibit a similar intensity throughout the NE and SW  
456 monsoonal periods for the Lupar river (Fig. 7a). This result could suggest that the occurrence of

457 extreme rainfall events, as reported for the year 2009, can exert a much larger impact on TSS  
458 transportation and release in monsoon-driven tropical rivers.

459 Drought events in 2014 can be seen to impact the precipitation values at both the Lupar (Fig. 7b) and  
460 Rajang river basins (Fig. 7d). There are no apparent patterns of decreasing precipitation values during  
461 the shift of NE to SW monsoonal periods as compared to the year 2009, for either river basin. However,  
462 precipitation values were found to increase sharply during the year end NE monsoon period for both  
463 river basins. The TSS concentrations at the Lupar coastal river points were found to be the highest  
464 during the NE monsoon period earlier in January and February of 2014 (Fig. 7b). This may be due to  
465 the temporal lag in the transition of TSS discharge into the coastal systems arising from the prior  
466 months (November and December) in the previous year, when higher rainfall events were typically  
467 observed in this region (Gomyo and Koichiro, 2009; Tangang et al., 2012). The TSS distribution at both  
468 Lupar and Rajang coastal river points showed no distinct trend in relation to the precipitation values  
469 throughout a period of ten months until November 2014. These findings suggest that coastal areas in  
470 the Borneo region may not be experiencing critical water quality degradation during dry seasons.

471

472

473

474

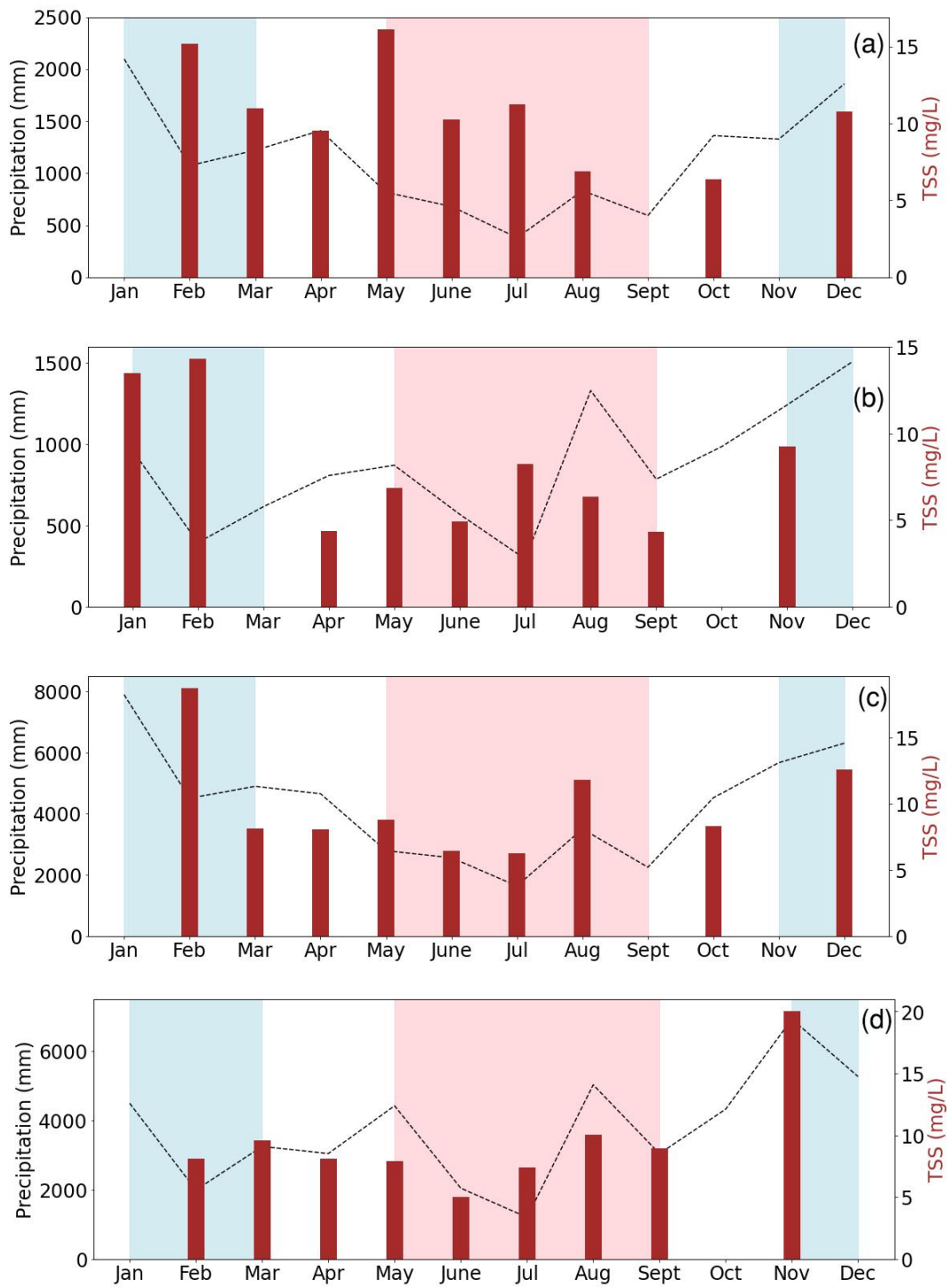
475

476

477

478





479

480 Fig. 7: Temporal analysis of precipitation (mm) from the Lupar and Rajang river basins in relation to TSS concentrations (mg/L)

481 during the NE and SW monsoon periods at the Lupar ((a): 2009; (c): 2014) and Rajang ((b): 2009; (d): 2014) coastal river point.

482 The NE monsoon months are highlighted with a blue background; those of the SW monsoon with a pink background, and

483 intermonsoon periods with a white background.



### 484 3.2.1 Temporal TSS anomalies

485 Considering the temporal variation recorded across monsoons, maps of relative TSS anomalies were  
486 calculated for each year as the difference with respect to the long-term TSS mean (Fig. 4), in order to  
487 detect changes of TSS distribution occurring annually (Fig. 8). As shown in Figure 8, year 2010  
488 experienced a distinct increase of TSS distribution (approximately 100 %), with widespread pattern  
489 extending into open ocean waters, in comparison to the long-term TSS mean. This finding provides an  
490 interesting insight into the effects of extreme rainfall events as recorded in year 2009, which could  
491 potentially intensify TSS release into the coastal and open ocean waters. The effects of TSS release  
492 can still be seen a year after the extreme rainfall events in this region. This observation could provide  
493 further evidence that the impacts of the TSS release from the land into rivers and coastal systems may  
494 only take effect after a substantial period, as previously observed by Sun et al. (2017a).

495 Figure 8 further reveals an interesting pattern of TSS increase in the Samunsam-Sematan region from  
496 year 2004 until 2019, with exceptions during the years 2007 and 2008. As previously highlighted in  
497 Section 3.1, the Samunsam-Sematan region has been observed to be a vulnerable coastal area with  
498 respect to TSS water quality degradation. From the annual map of TSS anomalies (Fig. 8), we can see  
499 that the TSS distribution has the tendency to accumulate in the Samunsam-Sematan region, as  
500 opposed to being distributed into the open ocean waters. This may be due to the geographical and  
501 hydrological characteristics of these coastal regions (Martin et al., 2018), as the TSS release may be  
502 sheltered from open ocean waters, and hence induce a higher TSS accumulation in these coastal  
503 regions.

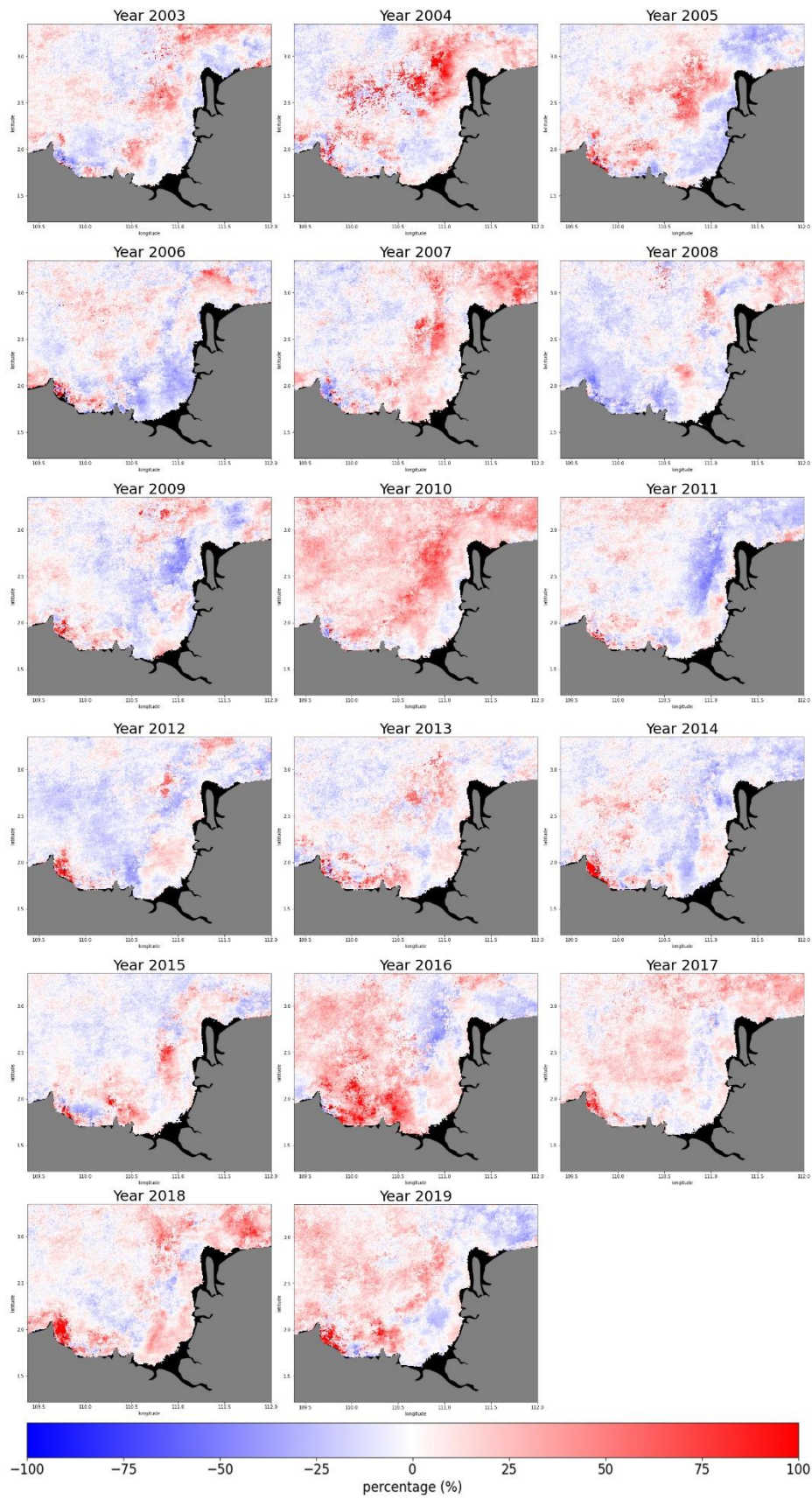
504

505

506

507

508



509

510 Fig. 8: Map of relative TSS distribution anomalies with respect to the long-term mean, represented as percentage (%), from  
 511 year 2003 until 2019.

512 3.3 Hydrological factors driving TSS discharge

513 Apart from the influence of monsoonal patterns, hydrological factors such as the river discharge are  
514 among the dominant drivers in transporting various water constituents in riverine and coastal systems  
515 (Loisel et al., 2014; Petus et al., 2014; Sun, 2017b; Verschelling et al., 2017). In this study, river  
516 discharge from the Lupar and Rajang basins was estimated and investigated.

517 Yearly river discharge estimates from 2003 until 2019 were investigated to assess its effect on the TSS  
518 distribution (Fig. 9) represented by changes in TSS values for pixels located at each Lupar and Rajang  
519 coastal river points (Supplementary Materials, Fig. S3). Figure 9a shows that river discharge values in  
520 the Lupar basin (750 to 1050 m<sup>3</sup>/s) are approximately twice lower than the Rajang river discharge (Fig.  
521 9b), which recorded a range of 3,200 to 4,000 m<sup>3</sup>/s.



522

523

524 Fig. 9: Time-series analysis of river discharge (m<sup>3</sup>/s) in relation to TSS concentrations (mg/L) for the Lupar (a) and Rajang (b)

525 basins from year 2003 to 2019. Note the differing scaling on the ordinate axes in each plot.

526

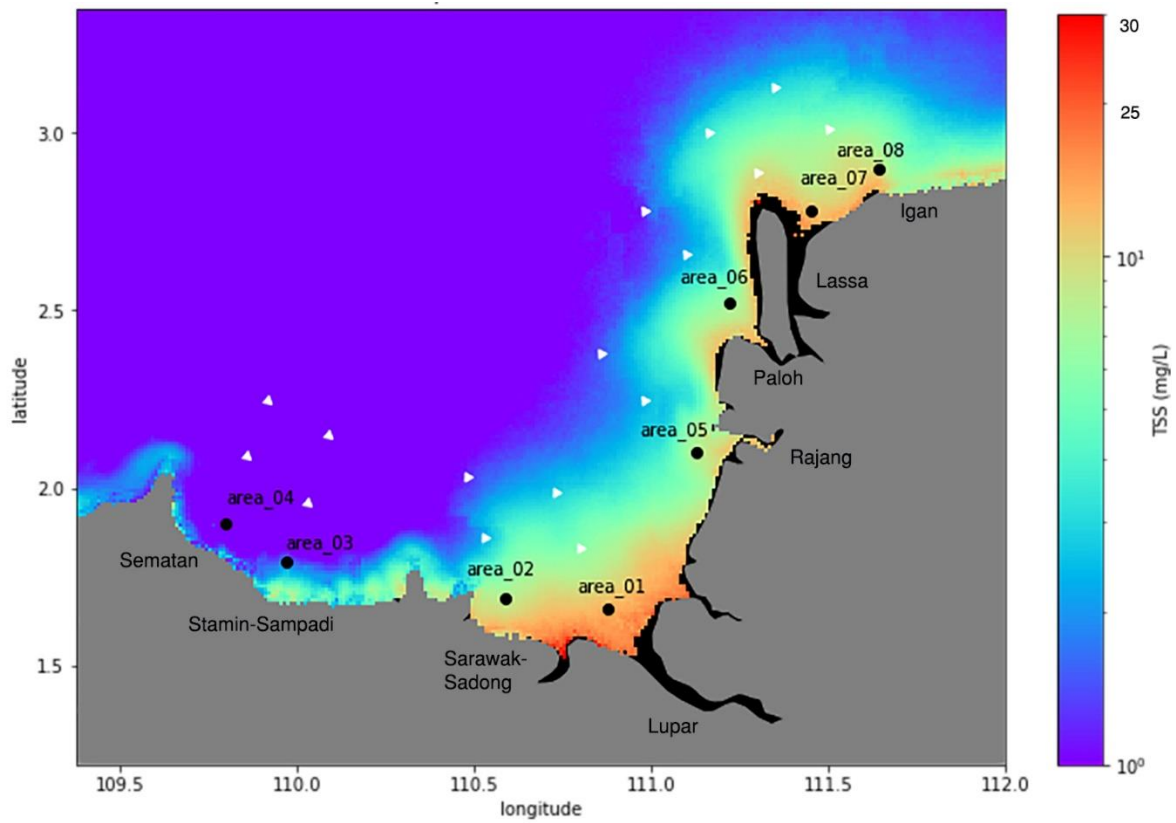
527 Discrepancies between TSS estimates and river discharge were identified in both the Lupar and Rajang  
528 coastal regions in these annual time-series, where river discharge was inversely correlated with TSS  
529 estimates. These discrepancies are not uncommon, as previously highlighted in a study by Zhan et al.  
530 (2019). Especially in 2010 for the Lupar river, Fig. 9a shows a drop in TSS release in relation to the  
531 steady increase of river discharge from the river basin. In 2011 and 2012, a negative correlation can  
532 be seen between river discharge and TSS estimates, while in subsequent years from 2013 until 2015,  
533 there is a clear positive correlation. The TSS output from the Lupar basin recorded a correlation  
534 coefficient of  $r = 0.15$ , while river discharge from the Rajang basin did not substantially influence the  
535 TSS release either, with  $r = 0.27$  throughout the seasons (Supplementary Materials, Fig. S8a and b).  
536 Although there is no obvious environmental factor that would explain these discrepancies and poor  
537 correlation between river discharge and TSS estimates in this study, these findings may imply a  
538 complex interaction and process between human interventions, such as damming and deforestation  
539 activities, which are largely occurring within the Rajang river basin (Alamgir et al., 2020), as well as  
540 varying hydrological and atmospheric conditions (wind and tidal mixing) in regulating TSS dynamics in  
541 a localised region (Espinoza Villar et al., 2013; Fabricius et al., 2016; Ramaswamy et al., 2004; Valerio  
542 et al., 2018; Wu et al., 2012; Zhan et al., 2019; Zhou et al., 2020).

#### 543 3.4 Variability of TSS across coastal waters

544 As previously observed in Fig. 4, varying river plumes of TSS were evidently detected within the coastal  
545 regions of the study area. Notably, coastal river plumes represent important factors driving the  
546 transport of water constituents and nutrients from coastlines to the open oceanic systems (Petus et  
547 al., 2014). To assess this and evaluate the water quality status in coastal zones, the spatial extent of  
548 TSS release was investigated along transects covering the territorial (12 nautical miles) and open water  
549 areas (24 nautical miles) of the Sarawak region (Fig. 10).

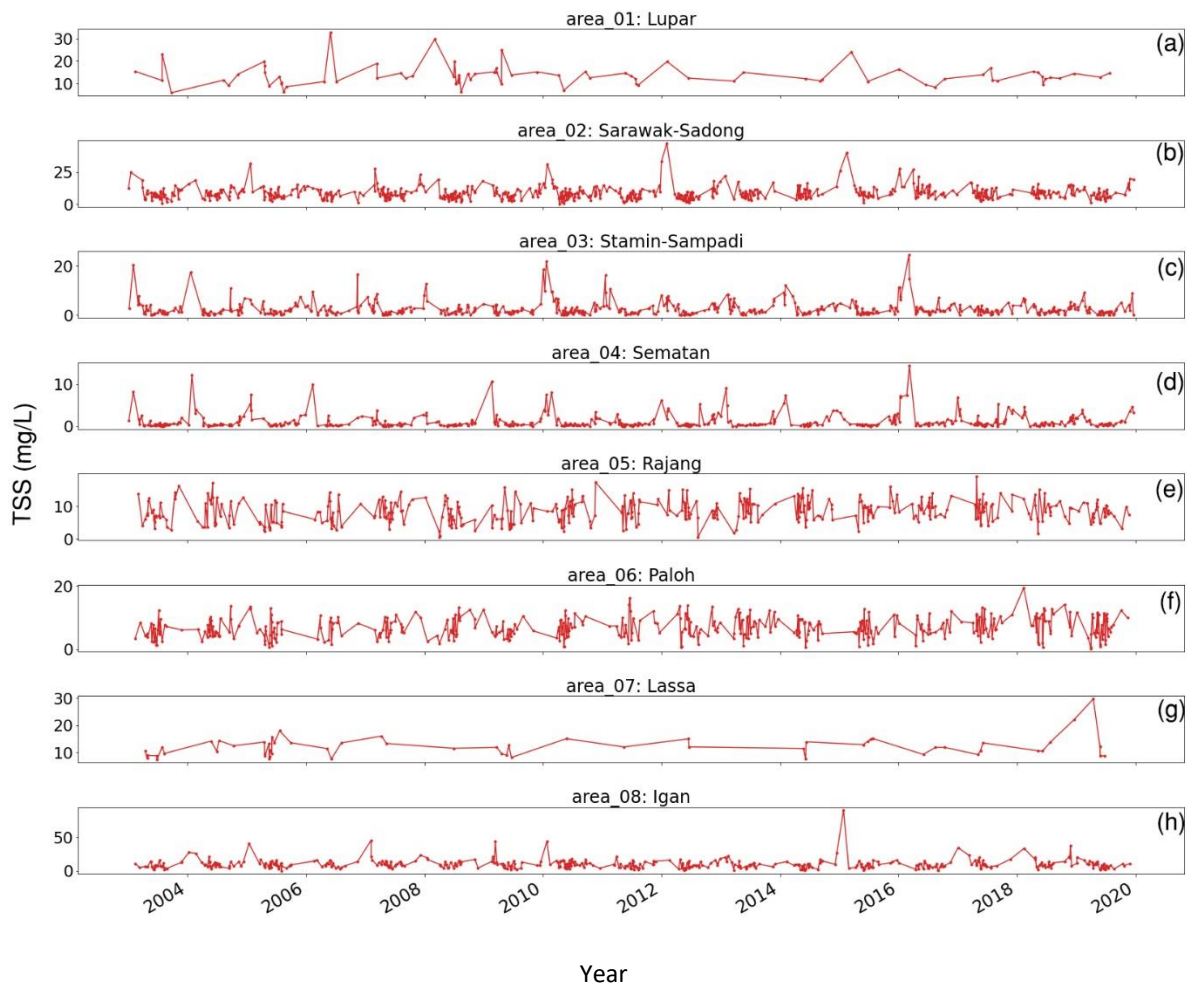
550 A total of eight coastal points were selected based on the main river mouths located in the southwest  
551 region of Sarawak. Transect points are positioned in a line starting at the coastal river points to

552 examine the variations of TSS distribution across different water zones. Daily changes in TSS  
553 concentration for each pixel located in front of the river mouths were plotted from 2003 until 2019  
554 (Fig. 11).



555

556 Fig. 10: Map of average TSS estimates (mg/L) with indicators at eight main river mouths and their transect, extending from  
557 coastal waters into territorial and open ocean systems. Indicators of each river mouths are as follows: area\_01 – Lupar river;  
558 area\_02 – Sarawak-Sadong river; area\_03 - Stamin-Sampadi river i; area\_04 – Sematan river; area\_05: Rajang river; area\_06:  
559 Paloh river; area\_07: Lassa river; and area\_08: Igan river).



560

561 Fig. 11: Graphs of daily TSS estimates (mg/L) recorded at eight river mouth points from 2003 to 2019. Presentation of each  
 562 river mouths is as follows: a) area\_01; b) area\_02; c) area\_03; d) area\_04; e) area\_05; f) area\_06; g) area\_07; h) area\_08.  
 563 Note the different TSS scales in each plot.

564 From the high temporal resolution graphs in Fig. 11, no general trend of TSS concentration can be  
 565 identified over the years at each coastal point. It is worth highlighting that the daily temporal  
 566 resolution was particularly affected at coastal points located in front of the Lupar (area\_01) and Lassa  
 567 (area\_07) river mouths due to various pixel data quality issues in these areas. Nonetheless, more than  
 568 80 satellite images with minimum cloud coverage at these two locations were processed, while the  
 569 remaining coastal points had a total of more than 400 satellite images to assess the temporal trend.

570 Despite the fact that no distinct upward or downward trend was observed, our findings indicate that  
 571 several river mouths are actively discharging and accumulating substantial TSS amounts over the

572 period of years, while resuspension of bottom sediments induced by wind and tidal cycle is another  
573 factor contributing to the variation of TSS values (Park, 2007; Song et al., 2020).

574 The coastal region of the Sarawak-Sadong river (area\_02) shows relatively high TSS distribution  
575 patterns with some periods recording an estimate of over 30 mg/L of TSS concentration. This is in  
576 agreement with the localised characteristics of the Sarawak river basin which essentially drains  
577 through the populated Kuching area with high industrial and development activities in the capital city  
578 of Sarawak (DID, 2021b). In comparison with other river mouth points, a steady TSS concentration  
579 below 20 mg/L was recorded across the Stamin-Sampadi (area\_03), Sematan (area\_04), Rajang  
580 (area\_05), and Paloh (area\_06) river mouths. Consistently high TSS values in the daily plots were  
581 recorded at the Lupar (area\_01) and Pulau Brait-Lassa (area\_07) river mouths, with estimates of up to  
582 30 mg/L on a near-daily basis. Similar high TSS amounts from the Igan (area\_08) river mouth, situated  
583 northeast side of the Pulau Brait-Lassa region, were observed in Cherukuru et al. (2021) and Staub et  
584 al. (2000).

585 Although the daily TSS estimates at each river point are in line with various reported studies (Chen et  
586 al., 2011, 2015b; Kim et al., 2017; Mungen et al., 2020; Zhang et al., 2010a), these estimates can be  
587 expected to be much higher for sampling points much closer to the river mouths. The selection of  
588 coastal river points in this study was made to minimize the gaps with respect to various pixel data  
589 quality issues in the MODIS-Aqua datasets, and hence, the use of coastal river points closer to shore  
590 would have been impractical.

591 These findings further suggest that higher TSS loadings within the coastal river areas would have been  
592 diluted or deposited while travelling to the open oceanic systems as they are weakly impacted by river  
593 discharge in relation to offshore distance (Espinoza Villar et al., 2013). This understanding can be  
594 observed in Fig. 12, which shows a progressively decreasing TSS estimates at each transect in relation  
595 to the distance from the shore. Generally, TSS estimates in coastal zones (first transect point) show  
596 considerably higher TSS concentrations. When moving outwards to territorial waters (second transect

597 point), TSS concentration estimates decrease by nearly 50 % before travelling to open ocean systems  
598 (third transect point), except for the northeast regions (area\_07 and area\_08) which seem to show  
599 large extension of TSS plumes to the open ocean waters, as also highlighted by Cherukuru et al. (2021).  
600 A reversed trend can be seen in the plot corresponding to the Sematan coastal river systems, although  
601 the absolute increase in TSS estimates across water zones (0.2 mg/L in total) here is only marginal (Fig.  
602 13d). Such slight trend in TSS retrievals recorded (Figure 12) generally offers a synoptic understanding  
603 of the trend conditions, considering such small variabilities in TSS retrieval were captured by the  
604 power function TSS retrieval model given its extent of uncertainties (Table 2).

605

606

607

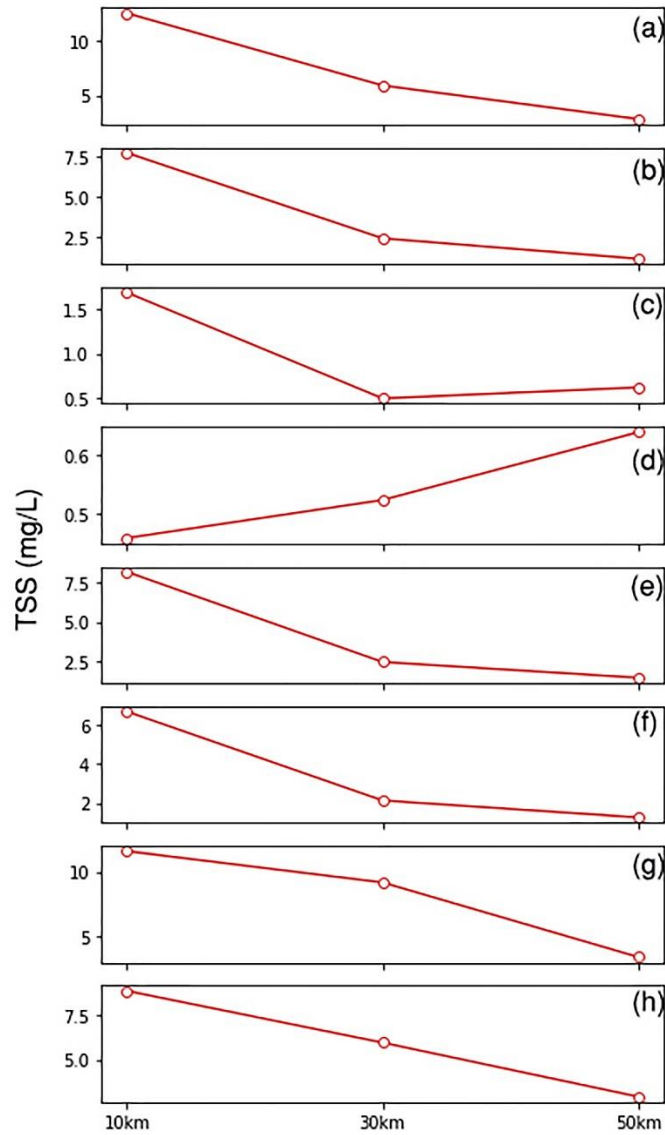
608

609

610

611





612

613 Fig. 12: Average TSS estimates (mg/L) computed from 2003 to 2019 for each of the eight rivers (area\_01: (a), area\_02: (b);  
 614 area\_03: (c); area\_04: (d); area\_05: (e); area\_06: (f); area\_07: (g); and area\_08: (h)) and their relevant transect points with  
 615 distance of 10 km (coastal waters), 30 km (territorial waters) and 50 km (open ocean waters) from the shoreline. Note the  
 616 varying TSS scales on the ordinate axes in each plot.

617

618

619

620

621 3.5 Discussion of TSS implications for coastal waters

622 High discharge of TSS into coastal environments can lead to adverse environmental and ecological  
623 implications. The presence of TSS affects water transparency and light availability within the surface  
624 waters (Dogliotti et al., 2015; Nazirova et al., 2021; Wang et al., 2021). Among others, TSS affects the  
625 photosynthesis activities of algae and macrophytes. TSS in water creates a reduction in light  
626 penetration, which impacts the primary production of aquatic organisms and hence the support  
627 system of marine life (Bilotta and Brazier, 2008; Loisel et al., 2014).

628 Additionally, TSS exerts an influence on zooplankton communities. Reduction in water clarity induces  
629 changes in the zooplankton's biomass volume and composition, while TSS may carry a level of toxicity  
630 which affects zooplankton through ingestion (Chapman et al., 2017; Donohue and Garcia Molinos,  
631 2009). Apart from that, accumulation and deposition of sediments decreases the level of dissolved  
632 oxygen (DO) at the bottom of the water column, and subsequently impacts the benthic invertebrate  
633 groups (Chapman et al., 2017). Moreover, substantial TSS deposition tends to cause harmful physical  
634 effects to these benthic groups, such as abrasion, and even clogging by sediment particles (Chapman  
635 et al., 2017; Langer, 1980).

636 As a result of these TSS effects on lower trophic levels, fish communities are critically impacted, with  
637 a reduction in diversity and abundance (Kemp et al., 2011). While fish communities learn to adapt to  
638 a range of TSS loads (Macklin et al., 2010), increase of TSS concentrations often depletes DO  
639 concentrations in the water system and causes stress towards these aquatic communities (Henley et  
640 al., 2000). Fish populations tend to decrease, as feeding and growth rates are negatively impacted  
641 (Shaw and Richardson, 2001; Sutherland and Meyer, 2007).

642 Threats to coral reefs have been linked to sediment-induced stress which often leads to a reduction  
643 in the coral's growth and metabolic rate, as well as impending mortality (Erftemeijer et al., 2012;  
644 Gilmour et al., 2006; Risk and Edinger, 2011). Factors of coral stress are driven by nutrient-rich  
645 sediments and microbes which are being carried by TSS, with impacts on the health of coral tissues

646 (Hodgson, 1990; Risk and Edinger, 2011; Weber et al., 2006). A reduction in light availability impedes  
647 the development of corals (Anthony and Hoegh-Guldberg, 2003; Rogers, 1979; Telesnicki and  
648 Goldberg, 1995). A combined increase in TSS and nutrient loadings contribute to the decrease of coral  
649 species diversity and composition (Fabricius, 2005).

650 Essentially, presence of TSS in water systems has impacts across various aquatic biota. With the severe  
651 implications of decreased fish population, this could lead to a disruption of fisheries activities by local  
652 communities, especially considering that more than 80 % of the Sarawak population is living in the  
653 coastal areas (DID, 2021a). Coral reefs are important coastal biodiversity assets to the Sarawak region,  
654 especially around the Talang-Talang and Satang islands on the southwest coast of Sarawak (Long,  
655 2014). With the use of remote sensing technologies in monitoring Sarawak coastal water quality, the  
656 approach presented in this paper provides digital-based solutions to assist relevant authorities and  
657 local agencies to better manage the Sarawak coastal waters and their resources.

#### 658 4.0 Conclusion

659 In this study, a regional empirical TSS retrieval model was developed to analyse TSS dynamics along  
660 the southwest coast of Sarawak. The empirical relationship between in situ reflectance values,  $R_{rs}(\lambda)$ ,  
661 and in situ TSS concentrations was established using a green-to-red band ratio using the MODIS-Aqua  
662  $R_{rs}(530)$  and  $R_{rs}(666)$  reflectance bands. An evaluation of the TSS retrieval model was carried out with  
663 error metric assessment, which yielded results of bias = 1.0, MAE = 1.47 and RMSE = 0.22 in mg/L  
664 computed in log<sub>10</sub>-transformed space prior to calculation. A statistical analysis using a k-fold cross  
665 validation technique (k = 7) reported low error metrics (RMSE = 0.2159, MAE = 0.1747).

666 The spatial TSS distribution map shows widespread TSS plumes detected particularly in the Lupar and  
667 Rajang coastal areas, with average TSS range of 15 – 20 mg/L estimated at these coastal areas. Based  
668 on the spatial map of the TSS coefficient of variation, large TSS variability was identified in the  
669 Samunsam-Sematan coastal areas (CV > 90 %). The map of temporal variation of TSS distribution  
670 points to a strong monsoonal influence in driving TSS release, with large differences identified

671 between the northeast and southwest monsoon periods in this region. From the annual TSS anomalies  
672 maps, the Samunsam-Sematan coastal areas demonstrated strong TSS variation spatially, while  
673 widespread TSS distribution with nearly 100 % of TSS increase in comparison to long term mean was  
674 observed in 2010. Furthermore, our study on river discharge in relation to TSS release demonstrated  
675 a weak relationship at both the Lupar and Rajang coastal river points. Study on the TSS variability  
676 across coastal river mouths implied that higher TSS loadings in the coastal areas are potentially being  
677 deposited or diluted in the process of being transported into the open ocean waters, with varying  
678 magnitude at several coastal river points.

679 Overall, these coastal areas of Sarawak are dominantly categorised as Class I quality, which remain  
680 within local quality standards to support various marine and socio-economic activities in this region.  
681 Our findings in the southwest coastal areas (Sematan and Stamin-Sampadi) showed that the coral  
682 reefs there can be well-maintained with negligible impacts from TSS loadings. However, it is important  
683 to highlight the various human activities that are widely ongoing in this region, which include  
684 deforestation and logging activities (Alamgir et al., 2020; Hon and Shibata, 2013; Vijith et al., 2018).  
685 Impacts from these activities in Sarawak can potentially aggravate current soil erosion issues, and  
686 ultimately induce more soil leaching and runoff from land to water systems, especially during heavy  
687 rainfall events (Ling et al., 2016; Vijith et al., 2018). As a result, human activities may have a greater  
688 influence on driving riverine sediments than climatological factors, as reported by Song et al. (2016).  
689 As such, this work presents the first observation of TSS distributions at large spatial and temporal  
690 scales in Sarawak's coastal systems, and of the potential associated impacts on the South China Sea.

691 While the findings derived from this work can be used to support local authorities in assessing TSS  
692 water quality status in the coastal areas of concern, the developed TSS retrieval model presents some  
693 limitations. Given the consideration that the model was developed from sediment and organic matter  
694 rich waters, the model is not transferable to other optical water types. This model is most applicable  
695 to be applied in waters with similar optical characteristics such as the southwest coastal waters of

696 Sarawak region. There is a need to further optimize the model with larger datasets covering more  
697 coastal water points, as well as data points from varied seasonal patterns, to improve its performance  
698 on a spatial and temporal scale. As these data points were collected within the southwest region of  
699 Sarawak's coastal waters, further testing and validation of the model in other regions of Sarawak's  
700 coastal waters is essential to develop a more robust TSS retrieval model and be applied to a broader  
701 regional scale.

702 Ultimately, with the demand to enhance coastal management and conservation strategies in  
703 Sarawak's coastal waters, the application of remote sensing technologies, as demonstrated in this  
704 study, is a great benefit in the development of sustainable sediment management in the Sarawak  
705 coastal region.

706 Data availability. The dataset related to this study is available as supplement to this paper.

707 Author contributions. Conceptualization, J.C., N.C., E.L., and M.M.; Formal analysis, J.C., N.C. and E.L.;  
708 Funding acquisition, M.M, N.C., and A.M.; Investigation, J.C., N.C., E.L., M.P., P.M., A.M., and M.M.;  
709 Methodology, J.C., N.C., E.L., and M.M.; Resources, J.C., N.C., E.L., M.P., and M.M.; Validation, J.C.,  
710 N.C., E.L. and M.M.; Writing— original draft, J.C.; Writing—review & editing, J.C., N.C., E.L., P.M., and  
711 M.M.; Supervision, M.M., N.C., and A.M.; Project administration, M.M., A.M., and N.C.

712 Competing interests. The authors declare that they have no conflict of interest.

713 Acknowledgement. We thank Sarawak Forestry Department and Sarawak Biodiversity Centre for  
714 permission to conduct collaborative research in Sarawak under permit numbers NPW.907.4.4(Jld.14)-  
715 161, SBC-RA-0097-MM, and Park Permit WL83/2017. We would like to extend our gratitude to all the  
716 boatmen and crew during all the field expeditions. Special thanks to Pak Mat and Minhad during the  
717 western region sampling, and Captain Juble, as well as Lukas Chin, during the eastern region cruises.  
718 We are appreciative to members of AQUES MY for their kind participation and involvement, especially  
719 to Ashleen Tan, Jack Sim, Florina Richard, Faith Chaya, Edwin Sia, Faddrine Jang, Gonzalo Carrasco,

720 Akhmetzada Kargazhanov, Noor Iskandar Noor Azhar, and Fakharuddin Muhamad. The study was  
721 supported by Australian Academy of Sciences under the Regional Collaborations Programme, Sarawak  
722 Multimedia Authority (Sarawak Digital Centre of Excellence) and Swinburne University of Technology  
723 (Swinburne Research Studentship).

724 References:

- 725 Ahn, Y. and Shanmugam, P.: Derivation and analysis of the fluorescence algorithms to estimate  
726 phytoplankton pigment concentrations in optically, , doi:10.1088/1464-4258/9/4/008, 2007.
- 727 Alamgir, M., Campbell, M. J., Sloan, S., Engert, J., Word, J. and Laurance, W. F.: Emerging challenges  
728 for sustainable development and forest conservation in Sarawak, Borneo, PLoS One, 15(3), 1–20,  
729 doi:10.1371/journal.pone.0229614, 2020.
- 730 Alcântara, E., Bernardo, N., Watanabe, F., Rodrigues, T., Rotta, L., Carmo, A., Shimabukuro, M.,  
731 Gonçalves, S. and Imai, N.: Estimating the CDOM absorption coefficient in tropical inland waters  
732 using OLI/Landsat-8 images, Remote Sens. Lett., 7(7), 661–670,  
733 doi:10.1080/2150704X.2016.1177242, 2016.
- 734 Anthony, K. R. N. and Hoegh-Guldberg, O.: Kinetics of photoacclimation in corals, Oecologia, 134(1),  
735 23–31, doi:10.1007/s00442-002-1095-1, 2003.
- 736 Babin, M., Stramski, D., Ferrari, G. M., Claustre, H., Bricaud, A., Obolensky, G. and Hoepffner, N.:  
737 Variations in the light absorption coefficients of phytoplankton, nonalgal particles, and dissolved  
738 organic matter in coastal waters around Europe, , 108, doi:10.1029/2001JC000882, 2003.
- 739 Bailey, S. W., Franz, B. A. and Werdell, P. J.: Estimation of near-infrared water-leaving reflectance for  
740 satellite ocean color data processing, Opt. Express, 18(7), 7521, doi:10.1364/oe.18.007521, 2010.
- 741 Balasubramanian, S. V., Pahlevan, N., Smith, B., Binding, C., Schalles, J., Loisel, H., Gurlin, D., Greb, S.,  
742 Alikas, K., Randla, M., Bunkei, M., Moses, W., Nguyễn, H., Lehmann, M. K., O’Donnell, D., Ondrusek,  
743 M., Han, T. H., Fichot, C. G., Moore, T. and Boss, E.: Robust algorithm for estimating total suspended  
744 solids (TSS) in inland and nearshore coastal waters, Remote Sens. Environ., 246(February), 111768,  
745 doi:10.1016/j.rse.2020.111768, 2020.
- 746 Bhardwaj, J., Gupta, K. K. and Gupta, R.: A review of emerging trends on water quality measurement  
747 sensors, Proc. - Int. Conf. Technol. Sustain. Dev. ICTSD 2015, (April), 1–6,  
748 doi:10.1109/ICTSD.2015.7095919, 2015.
- 749 Bilotta, G. S. and Brazier, R. E.: Understanding the influence of suspended solids on water quality and  
750 aquatic biota, Water Res., 42(12), 2849–2861, doi:10.1016/j.watres.2008.03.018, 2008.
- 751 Bong, C. H. J. and Richard, J.: Drought and climate change assessment using standardized  
752 precipitation index (Spi) for sarawak river basin, J. Water Clim. Chang., 11(4), 956–965,  
753 doi:10.2166/wcc.2019.036, 2020.
- 754 Brezonik, P. L., Olmanson, L. G., Finlay, J. C. and Bauer, M. E.: Factors affecting the measurement of  
755 CDOM by remote sensing of optically complex inland waters, Remote Sens. Environ., 157, 199–215,  
756 doi:10.1016/j.rse.2014.04.033, 2015.
- 757 Cao, F., Tzortziou, M., Hu, C., Mannino, A., Fichot, C. G., Del Vecchio, R., Najjar, R. G. and Novak, M.:  
758 Remote sensing retrievals of colored dissolved organic matter and dissolved organic carbon  
759 dynamics in North American estuaries and their margins, Remote Sens. Environ., 205(November

760 2017), 151–165, doi:10.1016/j.rse.2017.11.014, 2018.

761 Chapman, P. M., Hayward, A. and Faithful, J.: Total Suspended Solids Effects on Freshwater Lake  
762 Biota Other than Fish, *Bull. Environ. Contam. Toxicol.*, 99(4), 423–427, doi:10.1007/s00128-017-  
763 2154-y, 2017.

764 Chen, S., Huang, W., Chen, W. and Chen, X.: An enhanced MODIS remote sensing model for  
765 detecting rainfall effects on sediment plume in the coastal waters of Apalachicola Bay, *Mar. Environ.*  
766 *Res.*, 72(5), 265–272, doi:10.1016/j.marenvres.2011.09.014, 2011.

767 Chen, S., Han, L., Chen, X., Li, D., Sun, L. and Li, Y.: Estimating wide range Total Suspended Solids  
768 concentrations from MODIS 250-m imageries: An improved method, *ISPRS J. Photogramm. Remote*  
769 *Sens.*, 99, 58–69, doi:10.1016/j.isprsjprs.2014.10.006, 2015a.

770 Chen, S., Han, L., Chen, X., Li, D., Sun, L. and Li, Y.: Estimating wide range Total Suspended Solids  
771 concentrations from MODIS 250-m imageries: An improved method, *ISPRS J. Photogramm. Remote*  
772 *Sens.*, 99, 58–69, doi:10.1016/j.isprsjprs.2014.10.006, 2015b.

773 Chen, Z., Hu, C. and Muller-karger, F.: Monitoring turbidity in Tampa Bay using MODIS / Aqua 250-m  
774 imagery, , 109, 207–220, doi:10.1016/j.rse.2006.12.019, 2007.

775 Cherukuru, N., Ford, P. W., Matear, R. J., Oubelkheir, K., Clementson, L. A., Suber, K. and Steven, A.  
776 D. L.: Estimating dissolved organic carbon concentration in turbid coastal waters using optical  
777 remote sensing observations, *Int. J. Appl. Earth Obs. Geoinf.*, 52, 149–154,  
778 doi:10.1016/j.jag.2016.06.010, 2016a.

779 Cherukuru, N., Ford, P. W., Matear, R. J., Oubelkheir, K., Clementson, L. A., Suber, K. and Steven, A.  
780 D. L.: Estimating dissolved organic carbon concentration in turbid coastal waters using optical  
781 remote sensing observations, *Int. J. Appl. Earth Obs. Geoinf.*, 52, 149–154,  
782 doi:10.1016/j.jag.2016.06.010, 2016b.

783 Cherukuru, N., Martin, P., Sanwlani, N., Mujahid, A. and Müller, M.: A semi-analytical optical remote  
784 sensing model to estimate suspended sediment and dissolved organic carbon in tropical coastal  
785 waters influenced by peatland-draining river discharges off sarawak, borneo, *Remote Sens.*, 13(1), 1–  
786 31, doi:10.3390/rs13010099, 2021.

787 Chong, X. Y., Gibbins, C. N., Vericat, D., Batalla, R. J., Teo, F. Y. and Lee, K. S. P.: A framework for  
788 Hydrological characterisation to support Functional Flows (HyFFlow): Application to a tropical river,  
789 *J. Hydrol. Reg. Stud.*, 36(January), doi:10.1016/j.ejrh.2021.100838, 2021.

790 CIFOR: Forest Carbon Database, [online] Available from: <https://carbonstock.cifor.org/>, n.d.

791 Cui, T., Zhang, J., Groom, S., Sun, L., Smyth, T. and Sathyendranath, S.: Remote Sensing of  
792 Environment Validation of MERIS ocean-color products in the Bohai Sea : A case study for turbid  
793 coastal waters, *Remote Sens. Environ.*, 114(10), 2326–2336, doi:10.1016/j.rse.2010.05.009, 2010.

794 Davies, J., Mathew, U., Aikanathan, S., Nyon, Y. C. and Chong, G.: A Quick Scan of Peatlands, *Wetl.*  
795 *Int. Malaysia*, 1(March), 1–80, 2010.

796 Department of Environment: Malaysia Marine Water Quality Standards and Index, , 16 [online]  
797 Available from: <https://www.doe.gov.my/portalv1/wp-content/uploads/2019/04/BOOKLET-BI.pdf>  
798 (Accessed 12 September 2021), 2019.

799 Department of Statistics, M.: Sarawak Population, *Popul. by Adm. Dist. Ethn. group, Sarawak, 2020*  
800 [online] Available from: [https://sarawak.gov.my/web/home/article\\_view/240/175](https://sarawak.gov.my/web/home/article_view/240/175), 2020.

801 DID: Department of Irrigation & Drainage Sarawak: Introduction to Integrated Coastal Zone  
802 Management, [online] Available from: <https://did.sarawak.gov.my/page-0-123-476-INTEGRATED->

803 COASTAL-ZONE-MANAGEMENT.html (Accessed 21 October 2021a), 2021.

804 DID: Department Of Irrigation & Drainage Sarawak, 2021b.

805 Dindang, A., Chung, C. N. and Seth, S.: Heavy Rainfall Episodes over Sarawak during January-February  
806 2011 Northeast Monsoon, *JMM Res. Publ.*, (11), 41, 2011.

807 Dogliotti, A. I., Ruddick, K. G., Nechad, B., Doxaran, D. and Knaeps, E.: A single algorithm to retrieve  
808 turbidity from remotely-sensed data in all coastal and estuarine waters, *Remote Sens. Environ.*, 156,  
809 157–168, doi:10.1016/j.rse.2014.09.020, 2015.

810 Donohue, I. and Garcia Molinos, J.: Impacts of increased sediment loads on the ecology of lakes, *Biol.*  
811 *Rev.*, 84(4), 517–531, doi:10.1111/j.1469-185X.2009.00081.x, 2009.

812 Dorji, P. and Fearn, P.: Impact of the spatial resolution of satellite remote sensing sensors in the  
813 quantification of total suspended sediment concentration: A case study in turbid waters of Northern  
814 Western Australia, *PLoS One*, 12(4), 1–24, doi:10.1371/journal.pone.0175042, 2017.

815 Erftemeijer, P. L. A., Riegl, B., Hoeksema, B. W. and Todd, P. A.: Environmental impacts of dredging  
816 and other sediment disturbances on corals: A review, *Mar. Pollut. Bull.*, 64(9), 1737–1765,  
817 doi:10.1016/j.marpolbul.2012.05.008, 2012.

818 Espinoza Villar, R., Martinez, J. M., Le Texier, M., Guyot, J. L., Fraizy, P., Meneses, P. R. and Oliveira,  
819 E. de: A study of sediment transport in the Madeira River, Brazil, using MODIS remote-sensing  
820 images, *J. South Am. Earth Sci.*, 44, 45–54, doi:10.1016/j.jsames.2012.11.006, 2013.

821 European Space Agency: Sentinel-2, [online] Available from:  
822 <https://sentinels.copernicus.eu/web/sentinel/user-guides/sentinel-2-msi/> (Accessed 29 October  
823 2022a), 2022.

824 European Space Agency: Sentinel-3, [online] Available from:  
825 <https://sentinel.esa.int/web/sentinel/missions/sentinel-3> (Accessed 29 October 2022b), 2022.

826 Fabricius, K. E.: Effects of terrestrial runoff on the ecology of corals and coral reefs: Review and  
827 synthesis, *Mar. Pollut. Bull.*, 50(2), 125–146, doi:10.1016/j.marpolbul.2004.11.028, 2005.

828 Fabricius, K. E., Logan, M., Weeks, S. J., Lewis, S. E. and Brodie, J.: Changes in water clarity in  
829 response to river discharges on the Great Barrier Reef continental shelf: 2002-2013, *Estuar. Coast.*  
830 *Shelf Sci.*, 173, A1–A15, doi:10.1016/j.ecss.2016.03.001, 2016.

831 Gaveau, D. L. A., Sheil, D., Salim, M. A., Arjasakusuma, S., Ancrenaz, M., Pacheco, P. and Meijaard, E.:  
832 Rapid conversions and avoided deforestation : examining four decades of industrial plantation  
833 expansion in Borneo, *Nat. Publ. Gr.*, (September), 1–13, doi:10.1038/srep32017, 2016.

834 Gilmour, J. P., Cooper, T. F., Fabricius, K. E. and Smith, L. D.: Early warning indicators of change in the  
835 condition of corals and coral communities in response to key anthropogenic stressors in the Pilbara,  
836 Western Australia, *Aust. Inst. Mar. Sci. Rep. to Environ. Prot. Authority*. 101pp, 2006.

837 Giuliani, G., Chatenoux, B., Piller, T., Moser, F. and Lacroix, P.: Data Cube on Demand (DCoD):  
838 Generating an earth observation Data Cube anywhere in the world, *Int. J. Appl. Earth Obs. Geoinf.*,  
839 87(December 2019), 102035, doi:10.1016/j.jag.2019.102035, 2020.

840 Gomes, V. C. F., Carlos, F. M., Queiroz, G. R., Ferreira, K. R. and Santos, R.: Accessing and Processing  
841 Brazilian Earth Observation Data Cubes With the Open Data Cube Platform, *ISPRS Ann. Photogramm.*  
842 *Remote Sens. Spat. Inf. Sci.*, V-4–2021, 153–159, doi:10.5194/isprs-annals-v-4-2021-153-2021, 2021.

843 Gomyo, M. and Koichiro, K.: Spatial and temporal variations in rainfall and the ENSO-rainfall  
844 relationship over Sarawak, Malaysian Borneo, *Sci. Online Lett. Atmos.*, 5, 41–44,



845 doi:10.2151/sola.2009-011, 2009.

846 González Vilas, L., Spyarakos, E. and Torres Palenzuela, J. M.: Neural network estimation of  
847 chlorophyll a from MERIS full resolution data for the coastal waters of Galician rias (NW Spain),  
848 *Remote Sens. Environ.*, 115(2), 524–535, doi:10.1016/j.rse.2010.09.021, 2011.

849 Ha, N. T. T., Thao, N. T. P., Koike, K. and Nhuan, M. T.: Selecting the best band ratio to estimate  
850 chlorophyll-a concentration in a tropical freshwater lake using sentinel 2A images from a case study  
851 of Lake Ba Be (Northern Vietnam), *ISPRS Int. J. Geo-Information*, 6(9), doi:10.3390/ijgi6090290,  
852 2017.

853 Henley, W. F., Patterson, M. A., Neves, R. J. and Dennis Lemly, A.: Effects of Sedimentation and  
854 Turbidity on Lotic Food Webs: A Concise Review for Natural Resource Managers, *Rev. Fish. Sci.*, 8(2),  
855 125–139, doi:10.1080/10641260091129198, 2000.

856 Hodgson, G.: Tetracycline reduces sedimentation damage to corals, *Mar. Biol.*, 104(3), 493–496,  
857 1990.

858 Hon, J. and Shibata, S.: A Review on Land Use in the Malaysian State of Sarawak, Borneo and  
859 Recommendations for Wildlife Conservation Inside Production Forest Environment, *Borneo J.*  
860 *Resour. Sci. Technol.*, 3(2), 22–35, doi:10.33736/bjrst.244.2013, 2013.

861 Horsburgh, J. S., Spackman, A., Stevens, D. K., Tarboton, D. G. and Mesner, N. O.: Environmental  
862 Modelling & Software A sensor network for high frequency estimation of water quality constituent  
863 fluxes using surrogates, , 25, 1031–1044, doi:10.1016/j.envsoft.2009.10.012, 2010.

864 Howarth, R. W.: Coastal nitrogen pollution: A review of sources and trends globally and regionally,  
865 *Harmful Algae*, 8(1), 14–20, doi:10.1016/j.hal.2008.08.015, 2008.

866 Hu, C., Lee, Z. and Franz, B.: Chlorophyll a algorithms for oligotrophic oceans: A novel approach  
867 based on three-band reflectance difference, *J. Geophys. Res. Ocean.*, 117(1), 1–25,  
868 doi:10.1029/2011JC007395, 2012.

869 Jiang, D., Matsushita, B., Pahlevan, N., Gurlin, D., Lehmann, M. K., Fichot, C. G., Schalles, J., Loisel, H.,  
870 Binding, C., Zhang, Y., Alikas, K., Kangro, K., Uusõue, M., Ondrusek, M., Greb, S., Moses, W. J.,  
871 Lohrenz, S. and O’Donnell, D.: Remotely estimating total suspended solids concentration in clear to  
872 extremely turbid waters using a novel semi-analytical method, *Remote Sens. Environ.*, 258,  
873 doi:10.1016/j.rse.2021.112386, 2021.

874 Jiang, H. and Liu, Y.: Monitoring of TSS concentration in Poyang Lake based on MODIS data, *Yangtze*  
875 *River*, 42(17), 87–90, 2011.

876 Kemp, P., Sear, D., Collins, A., Naden, P. and Jones, I.: The impacts of fine sediment on riverine fish,  
877 *Hydrol. Process.*, 25(11), 1800–1821, doi:10.1002/hyp.7940, 2011.

878 Killough, B.: The Impact of Analysis Ready Data in the Africa Regional Data Cube, *Int. Geosci. Remote*  
879 *Sens. Symp.*, (July 2019), 5646–5649, doi:10.1109/IGARSS.2019.8898321, 2019.

880 Kim, H. C., Son, S., Kim, Y. H., Khim, J. S., Nam, J., Chang, W. K., Lee, J. H., Lee, C. H. and Ryu, J.:  
881 Remote sensing and water quality indicators in the Korean West coast: Spatio-temporal structures of  
882 MODIS-derived chlorophyll-a and total suspended solids, *Mar. Pollut. Bull.*, 121(1–2), 425–434,  
883 doi:10.1016/j.marpolbul.2017.05.026, 2017.

884 Krause, C., Dunn, B., Bishop-Taylor, R., Adams, C., Burton, C., Alger, M., Chua, S., Phillips, C., Newey,  
885 V., Kouzoubov, K., Leith, A., Ayers, D., Hicks, A. and DEA Notebooks contributors 2021: Digital Earth  
886 Australia notebooks and tools repository, , doi:https://doi.org/10.26186/145234, 2021.

887 Kuok, K. K., Chiu, P., Yap, A. and Law, K.: Determination of the Best Tank Model for the Southern

888 Region of Sarawak Determination Number of Tanks for Tank Model at Southern Region of Sarawak ,  
889 (August 2012), 2018.

890 Langer, O. E.: Effects of sedimentation on salmonid stream life, Environmental Protection Service.,  
891 1980.

892 Lavigne, H., Van der Zande, D., Ruddick, K., Cardoso Dos Santos, J. F., Gohin, F., Brotas, V. and  
893 Kratzer, S.: Quality-control tests for OC4, OC5 and NIR-red satellite chlorophyll-a algorithms applied  
894 to coastal waters, *Remote Sens. Environ.*, 255, 112237, doi:10.1016/j.rse.2020.112237, 2021.

895 Lee, K. H., Noh, J. and Khim, J. S.: The Blue Economy and the United Nations' sustainable  
896 development goals: Challenges and opportunities, *Environ. Int.*, 137(October 2019), 105528,  
897 doi:10.1016/j.envint.2020.105528, 2020a.

898 Lee, W. C., Viswanathan, K. K., Kamri, T. and King, S.: Status of Sarawak Fisheries: Challenges and  
899 Way Forward, *Int. J. Serv. Manag. Sustain.*, 5(2), 187–200, doi:10.24191/ijms.v5i2.11719, 2020b.

900 Lehner, B., Verdin, K. and Jarvis, A.: HydroSHEDS technical documentation, World Wildl. Fund US,  
901 Washington, DC, 1–27, 2006.

902 Lemley, D. A., Adams, J. B., Bornman, T. G., Campbell, E. E. and Deyzel, S. H. P.: Land-derived  
903 inorganic nutrient loading to coastal waters and potential implications for nearshore plankton  
904 dynamics, *Cont. Shelf Res.*, 174(August 2018), 1–11, doi:10.1016/j.csr.2019.01.003, 2019.

905 Lewis, A., Oliver, S., Lymburner, L., Evans, B., Wyborn, L., Mueller, N., Raevksi, G., Hooke, J.,  
906 Woodcock, R., Sixsmith, J., Wu, W., Tan, P., Li, F., Killough, B., Minchin, S., Roberts, D., Ayers, D.,  
907 Bala, B., Dwyer, J., Dekker, A., Dhu, T., Hicks, A., Ip, A., Purss, M., Richards, C., Sagar, S., Trenham, C.,  
908 Wang, P. and Wang, L. W.: The Australian Geoscience Data Cube — Foundations and lessons  
909 learned, *Remote Sens. Environ.*, 202, 276–292, doi:10.1016/j.rse.2017.03.015, 2017.

910 Limcih, F., Jilnm, M., Hb, H., Ilcach, H. N. M., Mnl, F., Fi, F. and Nb, F.: Study of Coastal Areas in Miri,  
911 in World Engineering Congress 2010, pp. 56–65., 2010.

912 Ling, T. Y., Soo, C. L., Sivalingam, J. R., Nyanti, L., Sim, S. F. and Grinang, J.: Assessment of the Water  
913 and Sediment Quality of Tropical Forest Streams in Upper Reaches of the Baleh River, Sarawak,  
914 Malaysia, Subjected to Logging Activities, *J. Chem.*, 2016, doi:10.1155/2016/8503931, 2016.

915 Liu, B., D'Sa, E. J. and Joshi, I.: Multi-decadal trends and influences on dissolved organic carbon  
916 distribution in the Barataria Basin, Louisiana from in-situ and Landsat/MODIS observations, *Remote  
917 Sens. Environ.*, 228(May), 183–202, doi:10.1016/j.rse.2019.04.023, 2019.

918 Loisel, H., Mangin, A., Vantrepotte, V., Dessailly, D., Ngoc Dinh, D., Garnesson, P., Ouillon, S.,  
919 Lefebvre, J. P., Mériaux, X. and Minh Phan, T.: Variability of suspended particulate matter  
920 concentration in coastal waters under the Mekong's influence from ocean color (MERIS) remote  
921 sensing over the last decade, *Remote Sens. Environ.*, 150, 218–230, doi:10.1016/j.rse.2014.05.006,  
922 2014.

923 Long, S. M.: Sarawak Coastal Biodiversity : A Current Status, *Kuroshio Sci.*, 8(1), 71–84 [online]  
924 Available from: <https://www.researchgate.net/publication/265793245>, 2014.

925 Lu, Y., Yuan, J., Lu, X., Su, C., Zhang, Y., Wang, C., Cao, X., Li, Q., Su, J., Ittekkot, V., Garbutt, R. A.,  
926 Bush, S., Fletcher, S., Wagey, T., Kachur, A. and Sweijid, N.: Major threats of pollution and climate  
927 change to global coastal ecosystems and enhanced management for sustainability, *Environ. Pollut.*,  
928 239, 670–680, doi:10.1016/j.envpol.2018.04.016, 2018.

929 Macklin, M. G., Jones, A. F. and Lewin, J.: River response to rapid Holocene environmental change:  
930 evidence and explanation in British catchments, *Quat. Sci. Rev.*, 29(13–14), 1555–1576,

931 doi:10.1016/j.quascirev.2009.06.010, 2010.

932 Mao, Z., Chen, J., Pan, D., Tao, B. and Zhu, Q.: A regional remote sensing algorithm for total  
 933 suspended matter in the East China Sea, *Remote Sens. Environ.*, 124, 819–831,  
 934 doi:10.1016/j.rse.2012.06.014, 2012.

935 Martin, P., Cherukuru, N., Tan, A. S. Y., Sanwlani, N., Mujahid, A. and Müller, M.: Distribution and  
 936 cycling of terrigenous dissolved organic carbon in peatland-draining rivers and coastal waters of  
 937 Sarawak, Borneo, *Biogeosciences*, 15(22), 6847–6865, doi:10.5194/bg-15-6847-2018, 2018.

938 Mengen, D., Ottinger, M., Leinenkugel, P. and Ribbe, L.: Modeling river discharge using automated  
 939 river width measurements derived from sentinel-1 time series, *Remote Sens.*, 12(19), 1–24,  
 940 doi:10.3390/rs12193236, 2020.

941 Milliman, J. D. and Farnsworth, K. L.: *River discharge to the coastal ocean: a global synthesis*,  
 942 Cambridge University Press., 2013.

943 Mohammad Razi, M. A., Mokhtar, A., Mahamud, M., Rahmat, S. N. and Al-Gheethi, A.: Monitoring of  
 944 river and marine water quality at Sarawak baseline, *Environ. Forensics*, 22(1–2), 219–240,  
 945 doi:10.1080/15275922.2020.1836076, 2021.

946 Morel, A. and Bélanger, S.: Improved detection of turbid waters from ocean color sensors  
 947 information, *Remote Sens. Environ.*, 102(3–4), 237–249, doi:10.1016/j.rse.2006.01.022, 2006.

948 Morel, A. and Gentili, B.: A simple band ratio technique to quantify the colored dissolved and detrital  
 949 organic material from ocean color remotely sensed data, *Remote Sens. Environ.*, 113(5), 998–1011,  
 950 doi:10.1016/j.rse.2009.01.008, 2009.

951 Mueller, J., Mueller, J., Pietras, C., Hooker, S., Clark, D., Frouin, A., Mitchell, B., Bidigare, R., Trees, C.  
 952 and Werdell, J.: *Ocean Optics Protocols For Satellite Ocean Color Sensor Validation, Revision 3*,  
 953 volumes 1 and 2., 2002.

954 Müller-dum, D., Warneke, T., Rixen, T., Müller, M., Baum, A., Christodoulou, A., Oakes, J., Eyre, B. D.  
 955 and Notholt, J.: Impact of peatlands on carbon dioxide ( CO 2 ) emissions from the Rajang River and  
 956 Estuary , Malaysia , , 17–32, 2019.

957 Müller, D., Warneke, T., Rixen, T., Müller, M., Mujahid, A., Bange, H. W. and Notholt, J.: Fate of  
 958 terrestrial organic carbon and associated CO<sub>2</sub> and CO emissions from two Southeast Asian estuaries,  
 959 *Biogeosciences*, 13(3), 691–705, doi:10.5194/bg-13-691-2016, 2016.

960 NASA official: Spectral Characterization Data by Sensor, [online] Available from:  
 961 [https://oceancolor.gsfc.nasa.gov/docs/rsr/rsr\\_tables/#MODIS-AQUA](https://oceancolor.gsfc.nasa.gov/docs/rsr/rsr_tables/#MODIS-AQUA) (Accessed 29 October 2022),  
 962 2022.

963 NASA Official: Ocean Level-2 Data Format Specification, [online] Available from:  
 964 <https://oceancolor.gsfc.nasa.gov/docs/format/l2nc/>, n.d.

965 Nazirova, K., Alferyeva, Y., Lavrova, O., Shur, Y., Soloviev, D., Bocharova, T. and Stochkov, A.:  
 966 Comparison of in situ and remote-sensing methods to determine turbidity and concentration of  
 967 suspended matter in the estuary zone of the mzymta river, black sea, *Remote Sens.*, 13(1), 1–29,  
 968 doi:10.3390/rs13010143, 2021.

969 Neil, C., Spyrakos, E., Hunter, P. D. and Tyler, A. N.: A global approach for chlorophyll-a retrieval  
 970 across optically complex inland waters based on optical water types, *Remote Sens. Environ.*,  
 971 229(May), 159–178, doi:10.1016/j.rse.2019.04.027, 2019.

972 Ondrusek, M., Stengel, E., Kinkade, C. S., Vogel, R. L., Keegstra, P., Hunter, C. and Kim, C.: The  
 973 development of a new optical total suspended matter algorithm for the Chesapeake Bay, *Remote*

974 Sens. Environ., 119, 243–254, doi:10.1016/j.rse.2011.12.018, 2012.

975 Open Data Cube: Open Data Cube, [online] Available from:  
976 <https://opendatacube.readthedocs.io/en/latest/user/intro.html> (Accessed 25 October 2021), 2021.

977 Pahlevan, N., Smith, B., Binding, C. and O'Donnell, D. M.: Spectral band adjustments for remote  
978 sensing reflectance spectra in coastal/inland waters, , 25(23), 2574–2591 [online] Available from:  
979 <http://arxiv.org/abs/1207.0580>, 2012.

980 Park, G. S.: The role and distribution of total suspended solids in the macrotidal coastal waters of  
981 Korea, Environ. Monit. Assess., 135(1–3), 153–162, doi:10.1007/s10661-007-9640-3, 2007.

982 Petus, C., Marieu, V., Novoa, S., Chust, G., Bruneau, N. and Froidefond, J. M.: Monitoring spatio-  
983 temporal variability of the Adour River turbid plume (Bay of Biscay, France) with MODIS 250-m  
984 imagery, Cont. Shelf Res., 74, 35–49, doi:10.1016/j.csr.2013.11.011, 2014.

985 Praveena, S. M., Siraj, S. S. and Aris, A. Z.: Coral reefs studies and threats in Malaysia: A mini review,  
986 Rev. Environ. Sci. Biotechnol., 11(1), 27–39, doi:10.1007/s11157-011-9261-8, 2012.

987 Ramaswamy, V., Rao, P. S., Rao, K. H., Thwin, S., Rao, N. S. and Raiker, V.: Tidal influence on  
988 suspended sediment distribution and dispersal in the northern Andaman Sea and Gulf of Martaban,  
989 Mar. Geol., 208(1), 33–42, doi:10.1016/j.margeo.2004.04.019, 2004.

990 Refaeilzadeh, P., Tang, L., Liu, H., Angeles, L. and Scientist, C. D.: Encyclopedia of Database Systems,  
991 Encycl. Database Syst., doi:10.1007/978-1-4899-7993-3, 2020.

992 Risk, M. J. and Edinger, E.: Impacts of sediment on coral reefs, Encycl. Mod. coral reefs. Springer,  
993 Netherlands, 575–586, 2011.

994 Rogers, C. S.: The effect of shading on coral reef structure and function, J. Exp. Mar. Bio. Ecol., 41(3),  
995 269–288, doi:10.1016/0022-0981(79)90136-9, 1979.

996 Sa'adi, Z., Shahid, S., Chung, E. S. and Ismail, T. bin: Projection of spatial and temporal changes of  
997 rainfall in Sarawak of Borneo Island using statistical downscaling of CMIP5 models, Atmos. Res.,  
998 197(November 2016), 446–460, doi:10.1016/j.atmosres.2017.08.002, 2017.

999 Sandifer, P. A., Keener, P., Scott, G. I. and Porter, D. E.: Oceans and Human Health and the New Blue  
1000 Economy, Elsevier Inc., 2021.

1001 Sarawak Forestry Corporation: Maludam National Park, [online] Available from:  
1002 <https://sarawakforestry.com/parks-and-reserves/maludam-national-park/>, 2022.

1003 Seegers, B. N., Stumpf, R. P., Schaeffer, B. A., Loftin, K. A. and Werdell, P. J.: Performance metrics for  
1004 the assessment of satellite data products: an ocean color case study, Opt. Express, 26(6), 7404,  
1005 doi:10.1364/oe.26.007404, 2018.

1006 Shaw, E. Al and Richardson, J. S.: Direct and indirect effects of sediment pulse duration on stream  
1007 invertebrate assemblages and rainbow trout (*Oncorhynchus mykiss*) growth and survival, Can. J.  
1008 Fish. Aquat. Sci., 58(11), 2213–2221, doi:10.1139/f01-160, 2001.

1009 Sim, C., Cherukuru, N., Mujahid, A., Martin, P., Sanwlani, N., Warneke, T., Rixen, T., Notholt, J. and  
1010 Müller, M.: A new remote sensing method to estimate river to ocean DOC flux in peatland  
1011 dominated Sarawak coastal regions, Borneo, Remote Sens., 12(20), 1–13, doi:10.3390/rs12203380,  
1012 2020.

1013 Siswanto, E., Tang, J. and Yamaguchi, H.: Empirical ocean-color algorithms to retrieve chlorophyll- a ,  
1014 total suspended matter , and colored dissolved organic matter absorption coefficient in the Yellow  
1015 and East China Seas, , 627–650, doi:10.1007/s10872-011-0062-z, 2011.

- 1016 Slonecker, E. T., Jones, D. K. and Pellerin, B. A.: The new Landsat 8 potential for remote sensing of  
 1017 colored dissolved organic matter (CDOM), *Mar. Pollut. Bull.*, 107(2), 518–527,  
 1018 doi:10.1016/j.marpolbul.2016.02.076, 2016.
- 1019 Song, C., Wang, G., Sun, X., Chang, R. and Mao, T.: Control factors and scale analysis of annual river  
 1020 water, sediments and carbon transport in China, *Sci. Rep.*, 6(May), 1–14, doi:10.1038/srep25963,  
 1021 2016.
- 1022 Song, Z., Shi, W., Zhang, J., Hu, H., Zhang, F. and Xu, X.: Transport mechanism of suspended  
 1023 sediments and migration trends of sediments in the central hangzhou bay, *Water (Switzerland)*,  
 1024 12(8), doi:10.3390/W12082189, 2020.
- 1025 Soo, C. L., Chen, C. A. and Mohd-Long, S.: Assessment of Near-Bottom Water Quality of  
 1026 Southwestern Coast of Sarawak, Borneo, Malaysia: A Multivariate Statistical Approach, *J. Chem.*,  
 1027 2017, doi:10.1155/2017/1590329, 2017.
- 1028 Soum, S., Ngor, P. B., Dilts, T. E., Lohani, S., Kelson, S., Null, S. E., Tromboni, F., Hogan, Z. S., Chan, B.  
 1029 and Chandra, S.: Spatial and long-term temporal changes in water quality dynamics of the tonle sap  
 1030 ecosystem, *Water (Switzerland)*, 13(15), doi:10.3390/w13152059, 2021.
- 1031 Staub, J. R. and Esterle, J. S.: Provenance and sediment dispersal in the Rajang River delta/coastal  
 1032 plain system, Sarawak, East Malaysia, *Sediment. Geol.*, 85(1–4), 191–201, doi:10.1016/0037-  
 1033 0738(93)90083-H, 1993.
- 1034 Staub, J. R., Among, H. L. and Gastaldo, R. A.: Seasonal sediment transport and deposition in the  
 1035 Rajang River delta, Sarawak, East Malaysia, *Sediment. Geol.*, 133(3–4), 249–264, doi:10.1016/S0037-  
 1036 0738(00)00042-7, 2000.
- 1037 Sun, C.: Riverine influence on ocean color in the equatorial South China Sea, *Cont. Shelf Res.*,  
 1038 143(December 2015), 151–158, doi:10.1016/j.csr.2016.10.008, 2017a.
- 1039 Sun, C.: Riverine influence on ocean color in the equatorial South China Sea, *Cont. Shelf Res.*,  
 1040 143(October 2016), 151–158, doi:10.1016/j.csr.2016.10.008, 2017b.
- 1041 Sutherland, A. B. and Meyer, J. L.: Effects of increased suspended sediment on growth rate and gill  
 1042 condition of two southern Appalachian minnows, *Environ. Biol. Fishes*, 80(4), 389–403,  
 1043 doi:10.1007/s10641-006-9139-8, 2007.
- 1044 Swain, R. and Sahoo, B.: Mapping of heavy metal pollution in river water at daily time-scale using  
 1045 spatio-temporal fusion of MODIS-aqua and Landsat satellite imageries, *J. Environ. Manage.*, 192, 1–  
 1046 14, doi:10.1016/j.jenvman.2017.01.034, 2017.
- 1047 Tangang, F. T., Juneng, L., Salimun, E., Sei, K. M., Le, L. J. and Muhamad, H.: Climate change and  
 1048 variability over Malaysia: Gaps in science and research information, *Sains Malaysiana*, 41(11), 1355–  
 1049 1366, 2012.
- 1050 Tawan, A. S., Ling, T. Y., Nyanti, L., Sim, S. F., Grinang, J., Soo, C. L., Lee, K. S. P. and Ganyai, T.:  
 1051 Assessment of water quality and pollutant loading of the Rajang River and its tributaries at Pelagus  
 1052 area subjected to seasonal variation and river regulation, *Environ. Dev. Sustain.*, 22(5), 4101–4124,  
 1053 doi:10.1007/s10668-019-00374-9, 2020.
- 1054 Telesnicki, G. J. and Goldberg, W. M.: CORAL REEF PAPER EFFECTS OF TURBIDITY ON THE  
 1055 PHOTOSYNTHESIS AND RESPIRATION OF TWO SOUTH FLORIDA REEF CORAL SPECIES portant factors  
 1056 in the regulation of coral cover , diversity , and abundance ( Ed- ships between suspended sediment  
 1057 concentrations or parti , , 57(2), 527–539, 1995.
- 1058 Tromboni, F., Dilts, T. E., Null, S. E., Lohani, S., Ngor, P. B., Soum, S., Hogan, Z. and Chandra, S.:

- 1059 Changing land use and population density are degrading water quality in the lower mekong basin,  
1060 Water (Switzerland), 13(14), 1–16, doi:10.3390/w13141948, 2021.
- 1061 United Nations: The Ocean Conference, in The Ocean Conference, vol. 53, p. 130, New York., 2017.
- 1062 Valerio, A. de M., Kappel, M., Vantrepotte, V., Ward, N. D., Sawakuchi, H. O., Less, D. F. D. S., Neu,  
1063 V., Cunha, A. and Richey, J.: Using CDOM optical properties for estimating DOC concentrations and  
1064 pCO<sub>2</sub> in the Lower Amazon River , Opt. Express, 26(14), A657, doi:10.1364/oe.26.00a657, 2018.
- 1065 Verschelling, E., van der Deijl, E., van der Perk, M., Sloff, K. and Middelkoop, H.: Effects of discharge,  
1066 wind, and tide on sedimentation in a recently restored tidal freshwater wetland, Hydrol. Process.,  
1067 31(16), 2827–2841, doi:10.1002/hyp.11217, 2017.
- 1068 Vijith, H., Hurmain, A. and Dodge-Wan, D.: Impacts of land use changes and land cover alteration on  
1069 soil erosion rates and vulnerability of tropical mountain ranges in Borneo, Remote Sens. Appl. Soc.  
1070 Environ., 12(September), 57–69, doi:10.1016/j.rsase.2018.09.003, 2018.
- 1071 Wang, C., Chen, S., Li, D., Wang, D., Liu, W. and Yang, J.: A Landsat-based model for retrieving total  
1072 suspended solids concentration of estuaries and coasts in China, Geosci. Model Dev., 10(12), 4347–  
1073 4365, doi:10.5194/gmd-10-4347-2017, 2017.
- 1074 Wang, J., Tong, Y., Feng, L., Zhao, D., Zheng, C. and Tang, J.: Satellite-Observed Decreases in Water  
1075 Turbidity in the Pearl River Estuary: Potential Linkage With Sea-Level Rise, J. Geophys. Res. Ocean.,  
1076 126(4), 1–17, doi:10.1029/2020JC016842, 2021.
- 1077 Weber, M., Lott, C. and Fabricius, K. E.: Sedimentation stress in a scleractinian coral exposed to  
1078 terrestrial and marine sediments with contrasting physical, organic and geochemical properties, J.  
1079 Exp. Mar. Bio. Ecol., 336(1), 18–32, doi:10.1016/j.jembe.2006.04.007, 2006.
- 1080 Werdell, P. J., McKinna, L. I. W., Boss, E., Ackleson, S. G., Craig, S. E., Gregg, W. W., Lee, Z.,  
1081 Maritorena, S., Roesler, C. S., Rousseaux, C. S., Stramski, D., Sullivan, J. M., Twardowski, M. S.,  
1082 Tzortziou, M. and Zhang, X.: An overview of approaches and challenges for retrieving marine  
1083 inherent optical properties from ocean color remote sensing, Prog. Oceanogr., 160, 186–212,  
1084 doi:10.1016/j.pocean.2018.01.001, 2018.
- 1085 Whitmore, T. C.: Tropical rain forests of the Par East, Oxford. Clarendon Press., 1984.
- 1086 Wilber, D. H. and Clarke, D. G.: Biological Effects of Suspended Sediments: A Review of Suspended  
1087 Sediment Impacts on Fish and Shellfish with Relation to Dredging Activities in Estuaries, North Am. J.  
1088 Fish. Manag., 21(4), 855–875, doi:10.1577/1548-8675(2001)021<0855:beossa>2.0.co;2, 2001.
- 1089 World Bank and United Nations Department of Economic and Social Affairs (UNDESA): The Potential  
1090 of the Blue Economy: Increasing Long-term Benefits of the Sustainable Use of Marine Resources for  
1091 Small Island Developing States and Coastal Least Developed Countries, World Bank, Washington DC.,  
1092 2017.
- 1093 Wu, C. S., Yang, S. L. and Lei, Y. ping: Quantifying the anthropogenic and climatic impacts on water  
1094 discharge and sediment load in the Pearl River (Zhujiang), China (1954-2009), J. Hydrol., 452–453,  
1095 190–204, doi:10.1016/j.jhydrol.2012.05.064, 2012.
- 1096 Yang, S. L., Zhao, Q. Y. and Belkin, I. M.: Temporal variation in the sediment load of the Yangtze river  
1097 and the influences of human activities, J. Hydrol., 263(1–4), 56–71, doi:10.1016/S0022-  
1098 1694(02)00028-8, 2002.
- 1099 Zhan, W., Wu, J., Wei, X., Tang, S. and Zhan, H.: Spatio-temporal variation of the suspended  
1100 sediment concentration in the Pearl River Estuary observed by MODIS during 2003–2015, Cont. Shelf  
1101 Res., 172(May 2018), 22–32, doi:10.1016/j.csr.2018.11.007, 2019.

1102 Zhang, L. J., Wang, L., Cai, W. J., Liu, D. M. and Yu, Z. G.: Impact of human activities on organic carbon  
1103 transport in the Yellow River, *Biogeosciences*, 10(4), 2513–2524, doi:10.5194/bg-10-2513-2013,  
1104 2013.

1105 Zhang, M., Tang, J., Dong, Q., Song, Q. T. and Ding, J.: Retrieval of total suspended matter  
1106 concentration in the Yellow and East China Seas from MODIS imagery, *Remote Sens. Environ.*,  
1107 114(2), 392–403, doi:10.1016/j.rse.2009.09.016, 2010a.

1108 Zhang, Y., Lin, S., Liu, J., Qian, X. and Ge, Y.: Time-series MODIS image-based retrieval and  
1109 distribution analysis of total suspended matter concentrations in Lake Taihu (China), *Int. J. Environ.*  
1110 *Res. Public Health*, 7(9), 3545–3560, doi:10.3390/ijerph7093545, 2010b.

1111 Zhou, Y., Xuan, J. and Huang, D.: Tidal variation of total suspended solids over the Yangtze Bank  
1112 based on the geostationary ocean color imager, *Sci. China Earth Sci.*, 63(9), 1381–1389,  
1113 doi:10.1007/s11430-019-9618-7, 2020.

1114

1115

1116

1117

1118

1119

1120

1121

1122

1123

1124

1125

1126

1127

1128

1129

1130